8-2014

DESIGN AND SIMULATION OF A NERVE TRACER SYSTEM FOR VAGOTOMY SURGERY

Guneet Bedi
Clemson University, gbedi@clemson.edu

DESIGN AND SIMULATION OF A NERVE TRACER SYSTEM FOR VAGOTOMY SURGERY

A Thesis
Presented to
the Graduate School of
Clemson University

In Partial Fulfillment
of the Requirements for the Degree
Master of Science
Electrical Engineering

---

by
Guneet Bedi
August 2014

Accepted by:
Dr. Timothy C. Burg, Committee Chair
Dr. David M. Kwartowitz
Dr. Rajendra Singh

Abstract

The vagus nerve is one of the most important nerves in the human body. It is associated with a plethora of functions one of them being acid secretion inside the stomach to aid in digestion. The cerebrum part of the brain initiates an action potential that is propagated along the vagus nerve to the parietal cells that secrete acid. In some cases, the cerebrum over stimulates the parietal cells leading to excess acid secretion, more than is needed for the digestion process. This excess acid leads to the formation of open sores along the stomach lining called gastric/peptic ulcers. In some cases, these gastric ulcers are curable by taking medicines. In other cases, medicines have little or no effect on these gastric ulcers and a surgical intervention, called a vagotomy is recommended to cure the gastric ulcers. Vagotomy is the surgical cutting of the vagus nerve branches that link the brain to the parietal cells that produce acid. Once a branch is cut, the signal from the cerebrum is blocked and acid production is reduced thereby reducing the formation of ulcers.

Vagotomy surgery can be challenging to perform. The major hurdle facing surgeons is locating the vagus nerve branch responsible for excess acid secretion in a specific zone of the stomach. If the surgeons are unable to locate the correct branch or cut other nerve branches, it will not cure the gastric ulcer problem and the entire surgical exercise may need to be revised. Thus there is a need to develop a system that would help surgeons locate and identify the

correct vagus nerve branch to cut during the vagotomy surgery. A system that artificially excites the vagus nerve and provides the surgeon feedback that the laparoscopic tool is near the vagus nerve branch of interest is proposed and designed.

To facilitate the design process, an external electrical stimulation model of a human vagus nerve was developed using COMSOL Multiphysics simulation software. The nerve model is built in the simulation software using the approximate geometric and material properties of the human vagus nerve. The model recapitulates the salient feature that if an applied electric potential exceeds a threshold potential, it leads to the generation of an action potential that propagates through the length of the vagus nerve.

The proposed vagus nerve tracer consists of a stimulation cuff to inject a trace signal into the vagus nerve and a receiver probe that can be placed near a nerve to detect the presence of the trace signal. The stimulation cuff is a set of copper electrodes that would be placed around the vagus nerve at a point above the stomach where the vagus nerve is clearly visible and accessible to the surgeons. The detector probe is designed as copper hook monopolar tip that could be affixed to a laparoscopic instrument. It can be placed around the vagus nerve branch without damaging it and can detect the action potential. An important third component is the square wave used as the trace signal.

The developed system thus comprises the vagus nerve artificial electrical stimulation cuff, trace signal, and detector probe. Computer simulations have been performed to optimize the proposed design and to demonstrate its functionality and potential value to help surgeons overcome the complication of locating the correct branch of vagus nerve to cut during the vagotomy surgery.

Table of Contents

Page

Table of Contents (Continued) **Page**

Table of Contents (Continued) **Page**

List of Figures

Figure **Page**

Figure **Page**

Figure **Page**

List of Tables

Table **Page**

CHAPTER 1

INTRODUCTION

1.1 Gastric Ulcers

A gastric ulcer is a defect in the stomach lining manifested as an open sore in the mucosal tissue that lines the stomach (Fig. 1.1) [1-3]. The number of people who suffer from gastric ulcers has been on the rise all around the world, nearly 25-30% of the world's population are affected by it [6]. The scope of this problem calls for improved remedies to cure this defect.

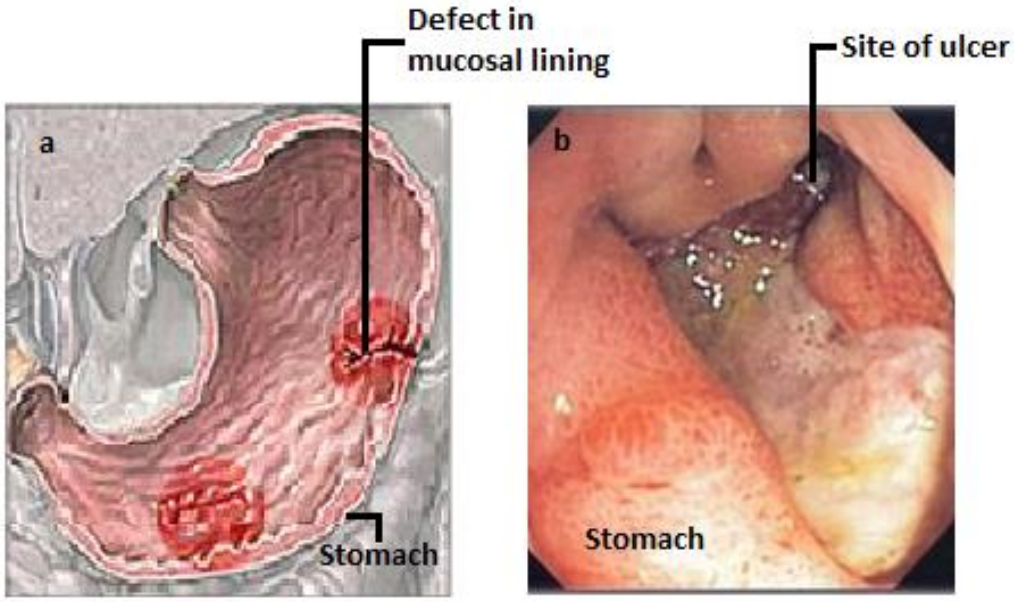

Fig.1.1. (a) Gastric ulcers illustration [3], **(b)** Photo of deep gastric ulcer [4].

Several factors may cause or contribute to gastric ulcers including bacterial (H.pylori) infection, drinking too much alcohol, smoking cigarettes or

chewing tobacco, regular use of aspirin, and increasing age. Some of the symptoms for gastric ulcers include abdominal pain, indigestion, nausea, and fatigue [5]. There are several forms of treatment available to address gastric ulcers. If the ulcer is caused by a bacterial infection, antibiotics are prescribed. If it is not a bacterial infection, antacids or antagonists are prescribed. If a patient doesn't respond to any of the medicines, then a surgical procedure called vagotomy is recommended [5]. In a vagotomy, the vagus nerve that conducts the signal from the brain to the parietal cells to increase gastric acid production in the stomach is cut. By doing so, the signal from the brain is blocked and acid production is reduced thereby reducing the formation of ulcers.

1.2 Nerve Cells and Behavior

Nerves are made up of nerve cells or neurons. They connect different parts of the body to the brain, forming a highly intricate system. The nerves can transmit signals from the brain to different parts of the body through motor neurons. The signal transmission can also take place in the reverse direction, i.e. from different parts of the body to the brain, through sensory neurons [7].

As illustrated in Fig. 1.2 neuron has the following main parts; a cell body (also known as soma), dendrites, axon and synapses. The cell body (soma) contains the nucleus. Dendrites are basically the signal receiving ends of the neuron. They pick up the electrical impulses from other nerve cells and transmit

them to the cell body. The axon is the signal transmitting part of the neuron. It receives electrical impulses from the cell body and transmits them to other nerve cells. Some axons have a fatty layer called a myelin sheath around them to speed up the electrical impulse transmission and also act as an insulator. Synapses are the connecting ends to other neurons or the point of communication between any two neurons. There is a small gap in between two neurons called a synaptic cleft [8], the synapses of the two neurons do not have to physically touch each other to communicate. Information is transferred from the presynaptic cell to the postsynaptic cells via neurotransmitters in the synaptic cleft.

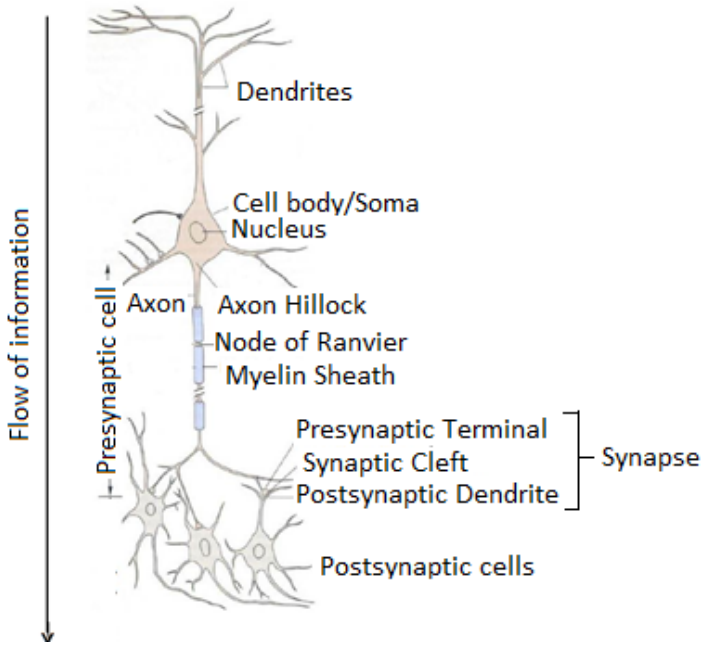

Fig.1.2. Structure of a Neuron [8].

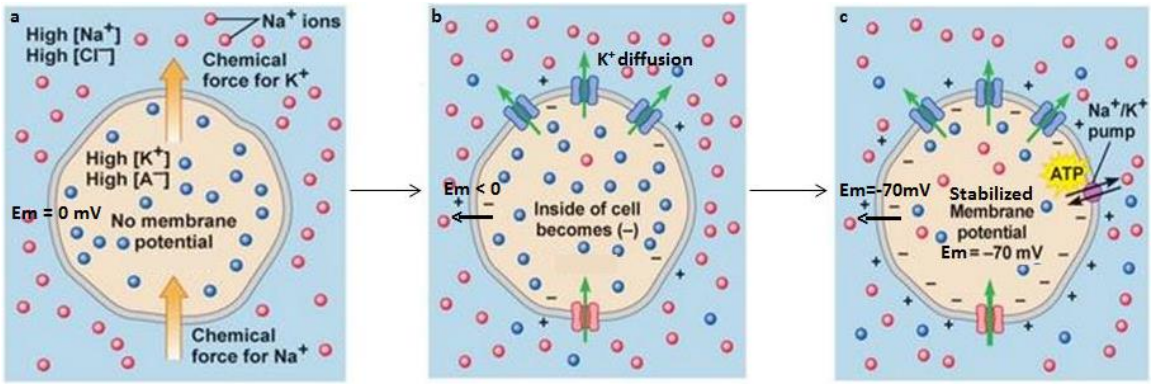

Fig.1.3 (a) Nerve cell ideal scenario, **(b)** K^+ diffuse out of the cell and membrane potential develops, **(c)** Na^+/K^+ pump counteracts the net loss of ions out of the cell maintaining the cell's resting potential [9]. A^- or anonymous ions are the remaining ions other than K^+, Na^+ or Cl^-.

A neuron ideally should have similar concentrations of sodium ions (Na^+) and potassium ions (K^+) across the cell membrane. Thus there should be no membrane potential on the neuron (Fig. 1.3(a)). In reality, the cell membrane is more permeable to K^+ than Na^+. Therefore, Na^+ flow rate into the cell is much slower than K^+ flow rate out of the cell. Since the inside of the cell is losing K^+ at a very rapid rate, it becomes more negative as compared to the outside. Thus a membrane potential develops (Fig. 1.3(b)). To stabilize the membrane voltage, the Na^+/K^+ pump acts. It counteracts the out flow of K^+ by actively pumping two K^+ inside the cell and three Na^+ out of the cell. This process reaches steady state at the cell's resting potential (Fig. 1.3(c)) between -70 and -90 mV [9]. Mathematically, the membrane potential E_m can be described by the Goldman equation [10]:

$$E_m = \frac{RT}{F} ln \left(\frac{\sum_i^N P_{ion_{i+}} \left[ion_i^+\right]_{out} + \sum_j^M P_{ion_{j-}} \left[ion_j^-\right]_{in}}{\sum_i^N P_{ion_{i+}} \left[ion_i^+\right]_{in} + \sum_j^M P_{ion_{j-}} \left[ion_j^-\right]_{out}} \right) \quad (1.1)$$

where

E_m = membrane potential (V)

$P_{ion_{i^+}}$, $P_{ion_{j^-}}$ = permeability for a given ion (m/s)

N = types of positive ion species present

M = types of negative ion species present

$[ion_i^+]_{out}$, $\left[ion_j^-\right]_{out}$ = extracellular concentration of given ion (mol/m^3)

$[ion_i^+]_{in}$, $\left[ion_j^-\right]_{in}$ = intracellular concentration of given ion (mol/m^3)

R = ideal gas constant = 8.3145 J K^{-1} mol^{-1}

T = absolute temperature (K)

F = Faraday's constant = 96485.3365 C mol^{-1}.

Action potentials are all-or-none nerve impulses that are initiated by a signal from the connecting nerve and arrive at the dendrites of the target nerve cell via neurotransmitters in the synapse (Fig. 1.2). These are rapid and transient by nature. Typically, action potentials have an amplitude of 100 mV and duration of about 1 ms [8]. If the membrane potential is rapidly depolarized i.e. it changes its polarity from a negative potential value to a positive potential value, and if this value is beyond a threshold value, an action potential is generated. This depolarization process is very brief (about 1 msec) and the membrane potential very quickly repolarizes to its original negative potential value. But an important

property of action potential is that once it is generated, it becomes self-propagating and propagates along the length of the axon at constant amplitude.

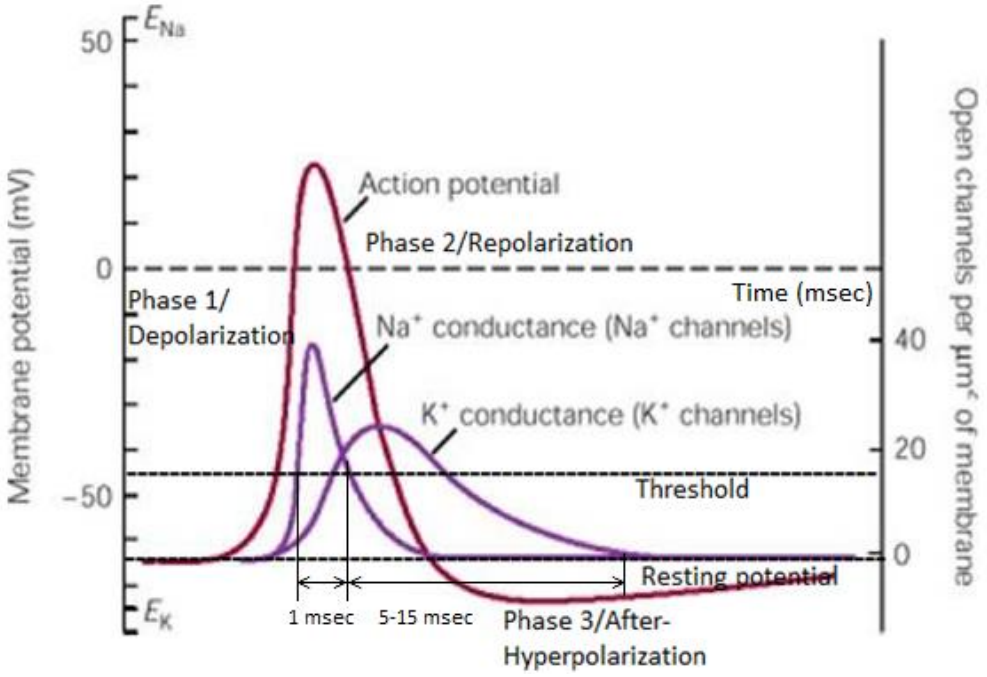

Fig.1.4. Generation of action potential due to Na^+ and K^+ conduction dynamics [8].

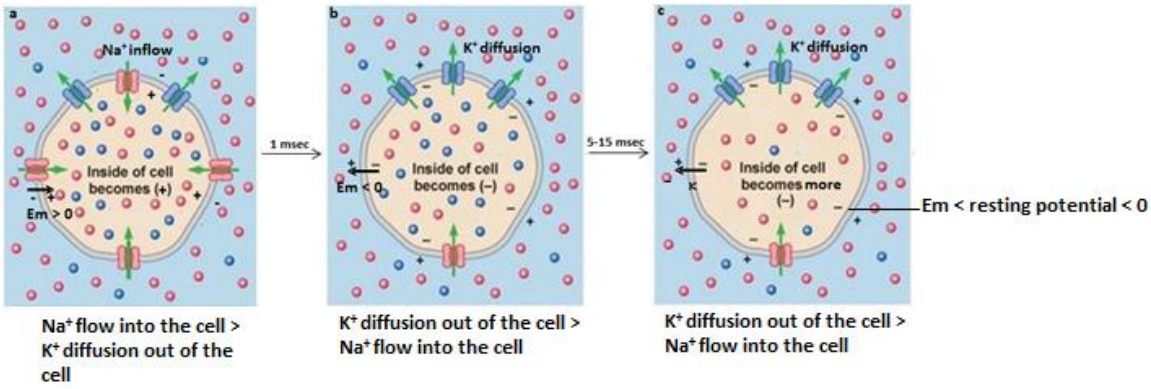

Fig.1.5 (a) Depolarization phase, **(b)** Repolarization phase, **(c)** After-hyperpolarization phase [9].

An action potential has three phases: depolarization, repolarization and after-hyperpolarization shown in Fig. 1.4 and Fig. 1.5. The first phase is the

depolarization phase in which the membrane Na^+ permeability increases more than the K^+ permeability. Due to this increase in permeability, the rate of Na^+ flow into the cell increases. The polarity of the membrane potential is reversed, $E_m>0$, since the inside of the cell is gaining Na^+ and as a result becoming more and more positive with respect to the outside of the cell. This phase is very brief (1msec) and almost instantly the permeability of the cell membrane to Na^+ decreases and to K^+ increases. This marks the beginning of phase two or the repolarization phase. This results in the diffusion of K^+ out of the cell, now the inside of the cell is losing K^+ at a very rapid rate, it becomes more negative as compared to the outside bringing the membrane potential back to its negative value. Now this phase is longer than phase one (5-15 msec), i.e. the permeability of the cell membrane towards K^+ remains high for a long time. As a result, the membrane potential overshoots the resting potential. This is phase three or the after-hyperpolarization phase [9].

1.3 Stimulation of Nerves and Neurons

Artificial electrical stimulation of neurons using electrode-based techniques has been used to study nerves for many years [11-13]. The reason for its utility is that these techniques provide flexibility to the user in terms of adjusting different parameters like current, voltage, and pulse duration. Also, the results obtained by employing these techniques are quite accurate and easily reproducible. A few application areas where the electrode based techniques are

employed currently are clinical applications like seizure control (Vagus Nerve Stimulation), deep brain stimulation and restoration of motor function [14-16]. Electrical stimulation, however, has a few inherent limitations including damage caused to the neuron due to intracellular electrodes and damage caused to the tissue due to extracellular electrodes. The damage may be mechanical i.e. caused due to friction between the electrode and the neuron or the tissue, or it may be electrical i.e. caused due to electrochemical reactions at the electrode-neuron or electrode-tissue interface.

1.4 Vagus Nerve

The vagus nerve is one of the longest and one of the most important nerve systems in a human body. “Vagus” is a Latin term that means “wandering”. It is also known by other names like pneumogastric nerve and cranial nerve X [17]. It originates at the brain and extends all the way down to the large intestines with several branches that innervate many organs lying in its path (Fig. 1.7). It is an important nerve as it contains both motor and sensory neurons [18] and connects to most internal organs in the human body through the numerous branches. For example, it connects to the heart through its cardiac branches, it connects to the lungs through its pulmonary branches, and it connects to the stomach through its gastric branches (Fig. 1.6). Thus, signals can be transmitted from the brain to all these organs and vice-a-versa through the vagus nerve. Since it innervates so many internal organs, it is associated with many high level

physiological functions: through the cardiac branches, it helps regulate heartbeat, through its pulmonary branches, it helps control muscle movement that affects breathing, and through its gastric branches it regulates acid secretion in stomach to aid digestion [19].

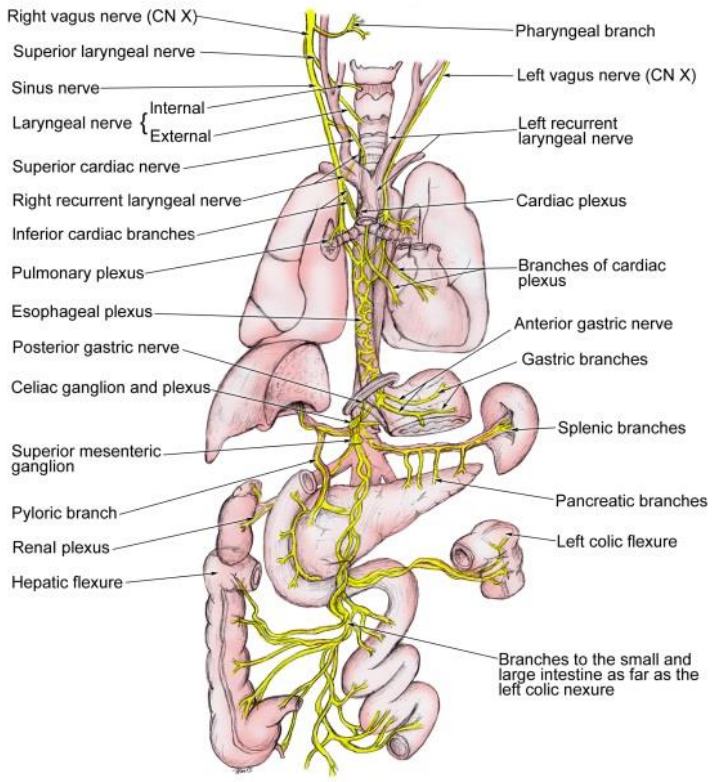

Fig.1.6. Vagus nerve branches [20].

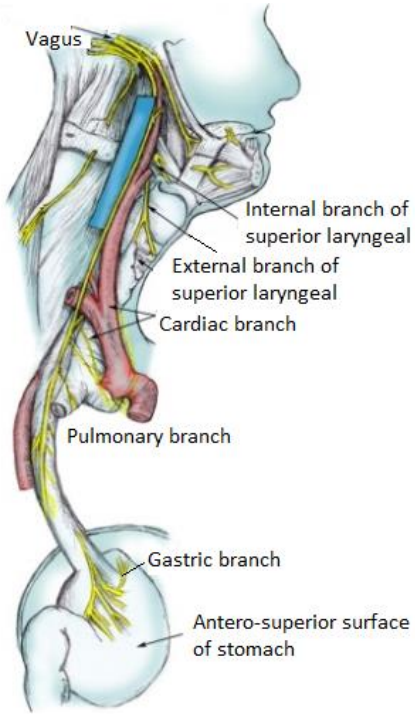

Fig.1.7. Course of the vagus nerve to the stomach [20].

1.5 Vagotomy

If too much acid is produced in the stomach, it may lead to formation of gastric ulcers along the lining of the stomach [6]. Vagotomy is the surgical cutting of the vagus nerve branches that link the brain to the parietal cells that produce acid as the means to reduce acid secretion in the stomach. If standard pharmacological treatments fail then a vagotomy may be recommended. By cutting the vagus nerve branch connecting the parietal cells, the signal from the brain is blocked and acid production is reduced thereby reducing the formation of ulcers.

On the basis of the location where the vagus nerve branch is cut, vagotomy can be classified as: truncal vagotomy, selective gastric vagotomy or selective proximal vagotomy (Fig. 1.8). If the vagus nerve branches to the stomach and intestines are cut, then this technique is called a truncal vagotomy. Since both the gastric branches and the intestinal branches are cut, impaired function beyond the targeted acid reduction may result from this low selectivity approach. If only the vagus nerve branches to the stomach are cut, then this technique is called selective gastric vagotomy. The selectivity in this case is slightly better than the truncal vagotomy as just the gastric branches are cut. The selectivity can be further increased if only the vagus nerve branches that innervate the acid-producing portion of the stomach are cut. This technique is called selective proximal vagotomy and is preferred over all other vagotomy techniques [21].

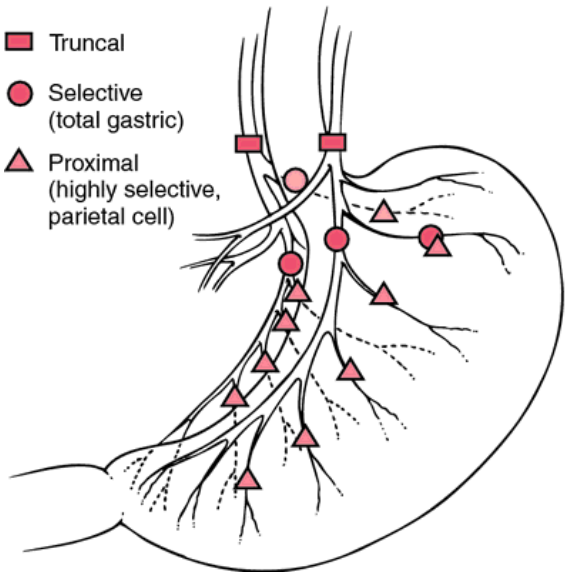

Fig.1.8. Vagotomy sites [22].

Laparoscopy or an open surgical procedure can be employed to perform a vagotomy [21]. Laparoscopy is often beneficial to the patient in terms of reduced pain and complications. The first step is to locate the exact position of the gastric ulcer. This is usually determined by taking a x-ray of the stomach. During the surgery, the surgeon makes an incision close to the abdominal region of the patient where he cuts the vagus nerve branches linking the parietal cells in the stomach. It can be complicated, at times, to locate the vagus nerve branches to cut as they might not be clearly identifiable or might be embedded in the tissue around the abdomen. Once the surgery is done, the surgeon sews back the abdominal muscles and the skin [6].

Like all surgical procedures, there are standard surgical risks associated with vagotomy. These include excessive bleeding and infection and gastric perforation. In addition to these standard surgical risks, some patients might experience delayed gastric emptying and dumping syndrome as side effects to vagotomy surgery. The recovery time from vagotomy surgery is around a week. A recovery period of around a month or two is generally required before a patient can resume all normal activities [6, 23].

1.6 Surgical Complications of Vagotomy: Project Motivation

Generally a vagotomy is quite effective in treating gastric ulcers. But still there are a few cases where individuals have complained of recurrence

of ulcers and had to undergo the entire surgical exercise again [21]. This shows that there is some complication in the surgery that is preventing the surgeons from achieving a 100% success rate in treating gastric ulcers. The major hurdle facing surgeons is locating the vagus nerve branch responsible for excess acid secretion in a specific zone of the stomach. This is majorly due to the fact that a high degree of variability exists in the numbers and location of the vagus nerve fibers in the human abdomen, making it extremely difficult to locate the complete and correct set of branches of the vagus nerve to cut. If the surgeons are unable to locate the correct branch or cut some other nerve branch, the gastric ulcers will not be cured and some other complication might arise as a result of cutting the wrong nerve branch. Thus there is a need to develop a system that would help surgeons locate and identify the correct vagus nerve branches to cut during the vagotomy surgery.

1.7 Vagus Nerve Stimulation (VNS) – An Existing System

The vagus nerve stimulation (VNS) system is used as a clinical application for seizure control to treat epilepsy. This VNS system is based on the concept of artificial external nerve stimulation.

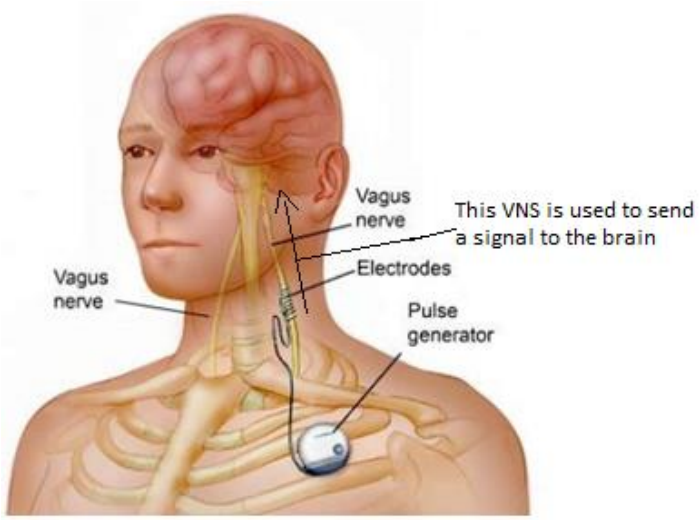

Fig.1.9. Vagus Nerve Stimulation [24].

As shown in Fig.1.9, the pulse generator is surgically placed under the skin in the upper chest. The electrode is attached to the vagus nerve branch in the neck and is connected to the pulse generator through a connecting wire running under the skin. Once the device is implanted in the patient, the pulse generator is programed to generate electrical pulses at regular intervals to stimulate the vagus nerve through the electrodes [24]. The major drawback of this current system is that it is expensive and invasive.

1.8 Overview of Proposed Vagus Nerve Tracing System

A system is proposed to help surgeons identify the vagus nerve branches while performing a vagotomy based on the concept of wringing connections in telephony and other complex wired networks. The fox and hound approach is to inject a trace into a wire of interest and then use probe to identify

the marked wire within a bundle. Here the vagus nerve is artificially stimulated (input) of a point before where the nerve needs to be cut and its effect (output) observed along the nerve (Fig.1.10.). If a detected signal correlates to the applied input e.g. frequency, then that means it is a vagus nerve that should potentially be cut. If no signal is observed at the output, then that means the nerve should not be cut. This way the surgeons can identify the correct vagus nerve with a greater degree of certainty. And the complications arising as a result of cutting the wrong nerve during vagotomy procedure could be reduced. The proposed vagus nerve tracing system would help the surgeons performing vagotomy to accurately identify the vagus nerve branches. Anyone with some basic knowledge and training should be able to operate the proposed vagus nerve tracing system.

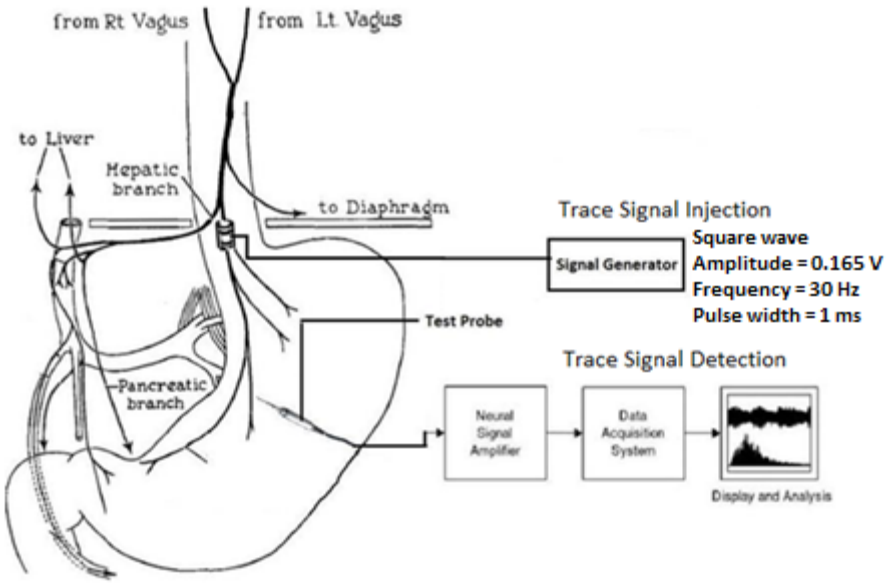

Fig.1.10. The proposed vagus nerve tracing system [25].

Safety is an important consideration in any nerve stimulation system, especially considering the functions served by the vagus nerve. The electrical pulse that is used to stimulate the vagus nerve should have a magnitude just sufficient enough to generate an action potential that propagates from its point of generation to the vagus nerve branch that needs to be cut. Moreover, this pulse is applied on the efferent vagus nerve i.e. the vagus nerve carrying signals from the brain towards an organ (in this case stomach). This way, the signal will not propagate in the reverse direction i.e. towards the cardiac branch or the brain once the vagus nerve is stimulated.

Chapter 2 contains the description of the design of the tracer signal and cuff electrodes. A 3D model of the human vagus nerve that serves as a test bed to study the generation and propagation of an action potential upon artificial electrical nerve stimulation is presented. The design of the tracer detector probes is described in chapter 3. In this chapter, different detector probe candidates are studied and a final candidate is shortlisted based on the end-use requirements. Chapter 4 includes the conclusions drawn from this research and suggests ideas for the next phase of the proposed system.

References

[1] “Peptic Ulcer”, http://www.nlm.nih.gov/medlineplus/ency/article/000206.htm, last accessed 07/19/2014.

[2] “Peptic Ulcer”, http://www.mayoclinic.com/health/peptic-ulcer/DS00242, last accessed 07/19/2014.

[3] “Peptic Ulcer”, http://www.nlm.nih.gov/medlineplus/pepticulcer.html, last accessed 07/19/2014.

[4] “Peptic Ulcer”, http://en.wikipedia.org/wiki/Peptic_ulcer, last accessed 07/19/2014.

[5] “Gastric Ulcer”, http://health.nytimes.com/health/guides/disease/gastric-ulcer/overview.html, last accessed 07/19/2014.

[6] “Vagotomy”, http://www.surgeryencyclopedia.com/St-Wr/Vagotomy.html#b, last accessed 07/19/2014.

[7] “Vagus Nerve”, http://www.newhealthguide.org/Vagus-Nerve.html, last accessed 07/19/2014.

[8] E.R. Kandel, J.H. Schwartz, and T.M. Jessell, Principles of Neural Science, McGraw-Hill (2000).

[9] “Nerve Cells and Electric Signaling”, http://droualb.faculty.mjc.edu/Course%20Materials/Physiology%20101/Chapter%20Notes/Fall%202011/chapter_7%20Fall%202011.htm, last accessed 07/19/2014.

[10] D. E. Haines and M. D. Ard, Fundamental neuroscience, Churchill Livingstone, New York (2002).

[11] G. Fritsch and J. E. Hitzig, Ueber die elektrische Erregbarkeit des Grosshirns, Veit, Leipzig (1870).

[12] L. A. Geddes and J. D. Bourland, "Tissue stimulation: theoretical considerations and practical applications," Med Biol Eng Comput 23(2), 131-137 (1985).

[13] J. K. Song, B. Abou-Khalil and P. E. Konrad, "Intraventricular monitoring for temporal lobe epilepsy: report on technique and initial results in eight patients," J Neurol Neurosurg Psychiatry 74(5), 561-565 (2003).

[14] N. Bhadra and P. H. Peckham, "Peripheral nerve stimulation for restoration of motor function," J Clin Neurophysiol 14(5), 378-393 (1997).

[15] D. A. Groves and V. J. Brown, "Vagal nerve stimulation: a review of its applications and potential mechanisms that mediate its clinical effects," Neurosci Biobehav Rev 29(3), 493-500 (2005).

[16] D. S. Kern and R. Kumar, "Deep brain stimulation," Neurologist 13(5), 237-252 (2007).

[17] “Vagus Nerve”, http://en.wikipedia.org/wiki/Vagus_nerve, last accessed 07/19/2014.

[18] “The Vagus Nerve”, http://www.bartleby.com/107/205.html, last accessed 07/19/2014.

[19] “Vagus Nerve”, http://www.md-health.com/Vagus-Nerve.html, last accessed 07/19/2014.

[20] Ted L Tewfik, “Vagus Nerve Anatomy”, http://emedicine.medscape.com/article/1875813-overview, last accessed 07/19/2014.

[21] “Vagotomy”, http://www.mdguidelines.com/vagotomy, last accessed 07/19/2014.

[22] “Vagotomy”, http://medical-dictionary.thefreedictionary.com/vagotomy, last accessed 07/19/2014.

[23] “What Is a Vagotomy?”, http://www.wisegeek.com/what-is-a-vagotomy.htm, last accessed 07/19/2014.

[24] “Vagus nerve stimulation”, http://www.whatisall.com/health/what-is-vagus-nerve-stimulation.html, last accessed 07/19/2014.

[25] R.G. Jackson, “Anatomy of the Vagus Nerves in the Region of the Lower Esophagus and the Stomach”, The Anatomical Record, Vol. 103 No. 1, January 1949.

CHAPTER 2

DESIGN OF THE TRACER SIGNAL AND TRACER EXCITATION CUFF

2.1 3D Modeling of a Human Vagus Nerve Test Bed

In order to optimize the design of the tracer excitation cuff, tracer signal, and tracer detector, a computer simulation of the system including a simulation test bed emulating a human vagus nerve branch was built. The simulation will be used to evaluate design choices for the tracer signal, tracer excitation cuffs, and tracer detector. The vagus nerve test bed is modeled and simulated using COMSOL 4.3b Multiphysics simulation software. The idea behind using this software was derived from the research paper in which a squid vagus nerve was simulated to study the action potential using an earlier version of COMSOL Multiphysics software [1].

2.1.1 COMSOL 4.3b Multiphysics Simulation

The AC/DC module and the Mathematics module of COMSOL Multiphysics was configured to model and simulate action potential generation and propagation through the vagus nerve test bed.

2.1.2 Vagus Nerve Test Bed Geometry

In this project, the 3D vagus nerve test bed geometry is defined in COMSOL using the available geometric entities and operations. It is first drawn in the Graphics window. The human vagus nerve axon is described as a hollow cylinder having a diameter ranging between 6 µm and 10 µm [5]. The vagus nerve comprises many such nerve axons bundled together and therefore can be approximated as a solid cylinder having a diameter ≈ 2 mm [6]. The maximum distance between the first and the last gastric branch is 13.5 cm [7] and can thus be taken as the length of the vagus nerve to be simulated. Fig. 2.1 shows the nerve model used in the simulation.

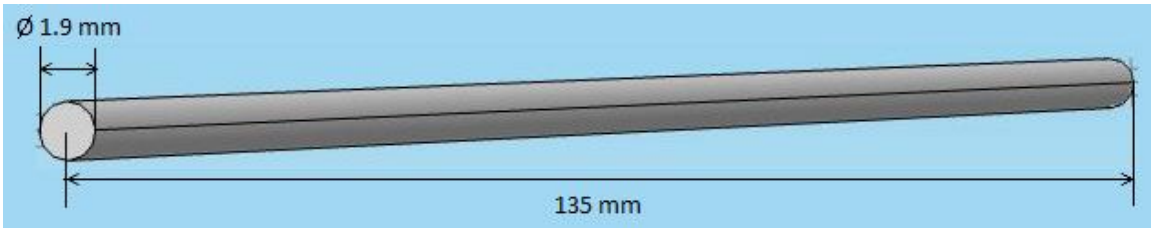

Fig. 2.1. Nerve model viewed in the Comsol graphics window

The next step is to surround the vagus nerve model with an extracellular medium. This is done to give the vagus nerve model the effect of an actual nerve inside a human body. This extracellular medium is modeled as a solid cylinder having a diameter 12 mm and the length 14.5 cm so that it uniformly covers the entire vagus nerve. Fig. 2.2 shows the extracellular medium surrounding the vagus nerve.

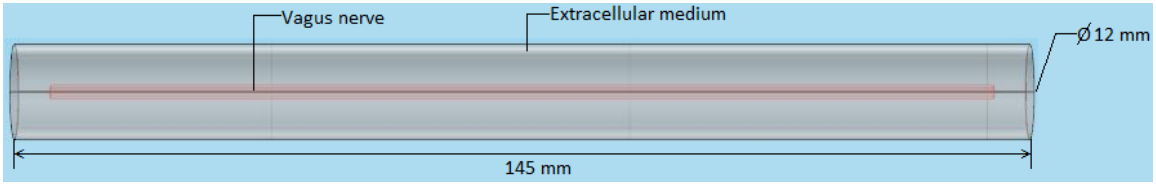

Fig. 2.2. Extracellular medium surrounding the vagus nerve (the nerve is shown in red).

2.1.3 Material

Predefined material data is available in COMSOL's material library and can be used to build different kinds of models with different material specifications [2]. When predefined material data is not available for a model, COMSOL provides flexibility to the user to create a custom or user-defined material by entering the desired material properties [2]. In this 3D vagus nerve test bed model, predefined materials are not available to model the vagus nerve or the extracellular medium. Hence, custom materials for both were created by specifying the desired material properties. Table 2.1 and Table 2.2 present the custom materials defined for the vagus nerve and the extracellular medium respectively.

PROPERTY	NAME	VALUE	UNIT
Electrical conductivity	sigma	0.18	S/m
Relative Permittivity	epsilonr	80	1

Table 2.1. User-defined vagus nerve material contents [11-13].

PROPERTY	NAME	VALUE	UNIT
Electrical conductivity	sigma	0.33	S/m
Relative Permittivity	epsilonr	80	1

Table 2.2. User-defined extracellular medium material contents [11-13].

2.1.4 Subdomain Settings

To design real-world systems, like the one designed in this project, multiphysics interactions may be needed. To model the vagus nerve, the different physics interfaces used are the electrostatics physics interface, found under AC/DC branch, for the extracellular medium model and PDE interface, found under Mathematics branch, for the vagus nerve model [2].

The Hodgkin-Huxley model has been employed for detailed study and analysis of several neuronal models [3]. This model is overly complicated for the work here as it involves solving four differential equations. A simpler model has been derived that brings down the number of differential equations to solve from four to just two, this model is called Fitzhugh-Nagumo model [15]. The Fitzhugh-Nagumo equations are given by:

$$\frac{\partial u_1}{\partial t} = (\propto -u_1)(u_1 - 1)u_1 + (-u_2) \tag{2.1}$$

$$\frac{\partial u_2}{\partial t} = \varepsilon(\beta u_1 - \gamma u_2 - \delta) \tag{2.2}$$

where,

$\propto$ = excitation threshold (V),

ε = excitability,

u_1 = excitation voltage in the neuron as a function of time,

u_2 = recovery processes of the resting potential,

β, γ, δ are parameters affecting the resting state and dynamics of the system.

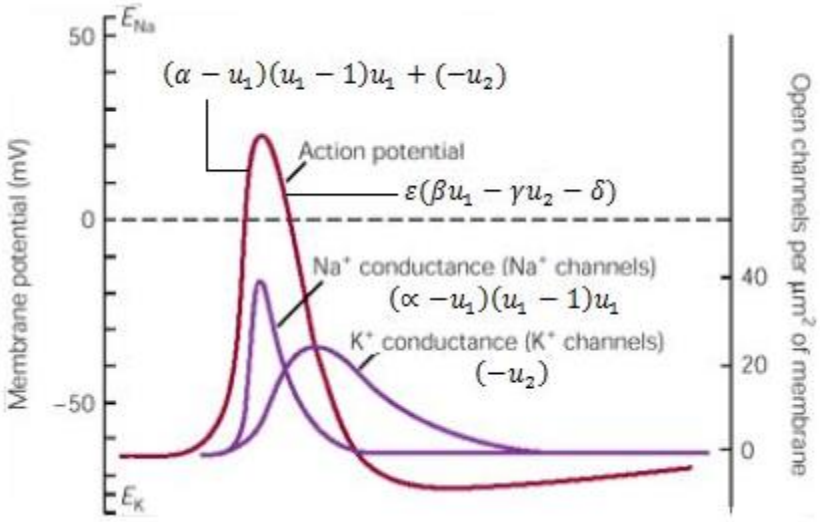

Fig. 2.3. Fitzhugh-Nagumo equations representing the change in membrane potential through the cycle of action potential generation and recovery [16].

The first differential equation (equation 2.1) in this model represents the change in membrane voltage due to the existence of sodium and potassium current dynamics in the cell. The second differential equation (equation 2.2) in this model represents the membrane potential recovery process (Fig 2.3). Excitation threshold $\propto$ is responsible for the firing of the action potential. An action potential is only generated if the initial applied voltage V_0 is above the excitation threshold $\propto$ (Fig. 2.4), typically $\propto$ = 0.1 V. Excitability ε affects the system in a way that if

the value of excitability is large ($\varepsilon \geq 0.03$), the action potential will die out prematurely i.e. it will not reach its peak value (Fig. 2.5). Typically $\varepsilon = 0.01$ [15].

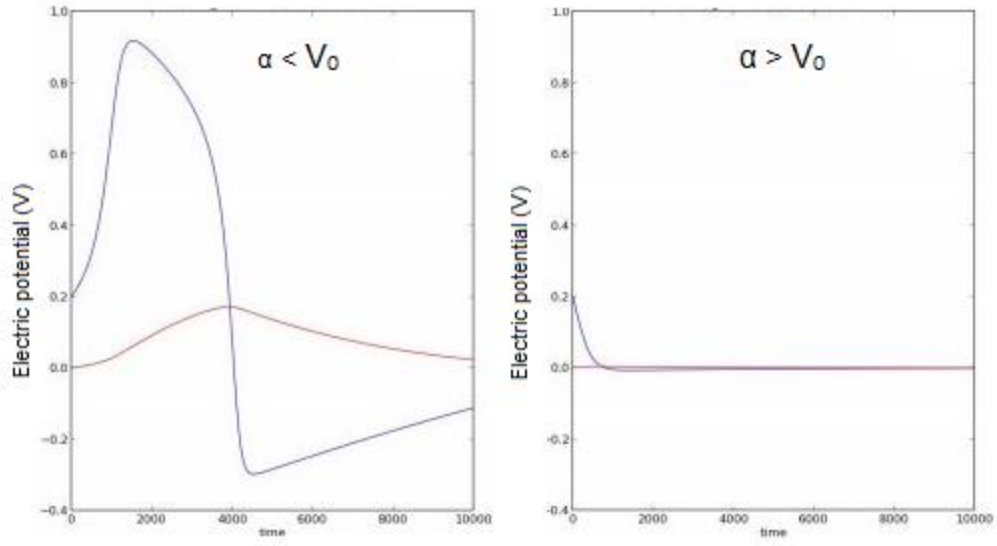

Fig. 2.4. Effect of excitation threshold on action potential [15].

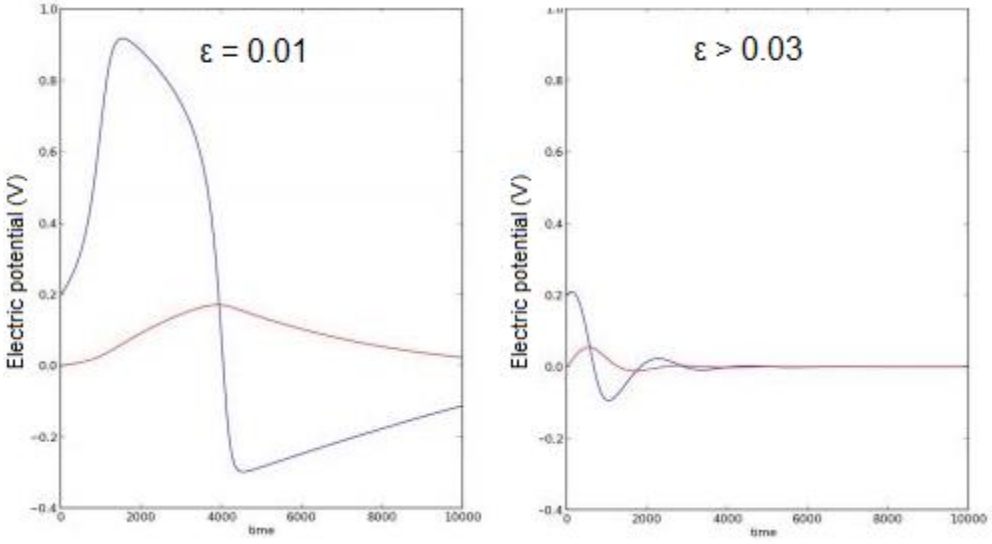

Fig. 2.5. Effect of excitability on action potential [15].

In COMSOL Multiphysics, the general form PDE physics interface is used to describe the vagus nerve model using the Fitzhugh-Nagumo equations. In this case, the vagus nerve is the sub-domain and u_1 and u_2 are the dependent variables. The external medium is inactive. The following equations are defined in the PDE physics interface of COMSOL Multiphysics [2]:

$$e_a \frac{\partial^2 u}{\partial t^2} + d_a \frac{\partial u}{\partial t} + \nabla . \Gamma = f \tag{2.3}$$

$$u = [u_1, u_2]^T \tag{2.4}$$

$$\nabla = \left[\frac{\partial}{\partial x}, \frac{\partial}{\partial y}, \frac{\partial}{\partial z}\right] \tag{2.5}$$

where,

e_a = mass coefficient,

d_a = damping coefficient,

Γ => $\Gamma_1 = \begin{bmatrix} -u_1 x \\ -u_1 y \\ -u_1 z \end{bmatrix}$, $\Gamma_2 = \begin{bmatrix} 0 \\ 0 \\ 0 \end{bmatrix}$ = conservative flux vector, and

f = source term for Fitzhugh-Nagumo equation

To obtain the Fitzhugh-Nagumo equations (equations (2.1) and (2.2)) from the predefined PDE physics interface equations (equations (2.3), (2.4) and (2.5)), the following values should be assigned to the parameters: e_a = 0, d_a = 1, which are obtained by comparing the two sets of equations. Γ_1 is left to its default values for u_1 i.e. $-u_1 x$, $-u_1 y$ and $-u_1 z$ representing the negative gradient of u_1 and Γ_2 = 0. The source term f is assigned the following values:

$$f_1 = (\alpha - u_1)(u_1 - 1)u_1 + (-u_2) \tag{2.6}$$

$$f_2 = \varepsilon(\beta u_1 - \gamma u_2 - \delta) \tag{2.7}$$

To generate the action potential, the following initial values are assigned to u_1 and u_2:

$$u_1 = V_0\big((x + d) > 0\big)((z + d) > 0) \tag{2.8}$$

$$u_2 = nu_0\big((-x + d) > 0\big)((z + d) > 0) \tag{2.9}$$

The values used for the parameters in the equations above have been tabulated in Table 2.3.

DESCRIPTION	NAME	VALUE	UNIT
Excitation threshold	α	0.1	V
System parameter	β	0.75	1
System parameter	γ	1	1
System parameter	δ	0	1
Excitability	ε	0.01	1
Elevated potential	V_0	0.165	V
Elevated relaxation value	nu_0	0.0025	V
Off-axis shift distance	d	1	mm

Table 2.3. Parameter Values for Fitzhugh-Nagumo equations used in the simulation [13].

For the extracellular medium, the electrostatic physics interface is used. In this case, the extracellular medium is the subdomain and V is the

dependent variable. The electrostatics physics interface is found under the AC/DC branch of COMSOL Multiphysics, which solves the following equations:

$$\nabla . D = \rho_v \tag{2.10}$$

$$E = -\nabla V \tag{2.11}$$

where,

V = electric potential = V_0 (V)

D = electric displacement (C/m^2)

E = electric field (V/m)

ρ = spatial charge density = 0 C/m^3 .

The constitutive relation between electric field, E and electric displacement, D is given by the following equation:

$$D = \varepsilon_0 \varepsilon_r E \tag{2.12}$$

where,

ε_0 = permittivity of vacuum and

ε_r = relative permittivity.

The initial value of the dependent variable being solved, V is taken to be 0 V (default value).

2.1.5 Boundary Conditions

The potential distribution in the extracellular medium can be described using the electrostatic form of Maxwell's equation and is solved using the Finite Element Method (FEM). The behavior of the vagus nerve can be described using the general form of partial differential equations and these equations are solved using the non-linear solver [2]. There are two solutions available for the two different elements of our simulation. To achieve an overall understanding of the working of the simulated vagus nerve, the two solutions must be combined. Using COMSOL Multiphysics 4.3b, one can couple the solution obtained for the potential distribution with the result from the non-linear solver. This kind of coupling can be achieved by setting the boundary conditions (BC) [2].

In the PDE subdomain, all boundaries of the vagus nerve are considered as Neumann boundaries. The following equations are used to set the boundary conditions that satisfy these Neumann boundaries.

$$-n \cdot \Gamma = G \tag{2.13}$$

where,

n = normal vector

Γ = numerical flux

G = source term for Neumann boundary condition.

For this simulation, Γ has the same value as set above for Γ_1 and Γ_2. The source term, G however is 0 (default). Therefore, equation (2.13) can be re-written as:

$$-n \cdot \Gamma = 0. \tag{2.14}$$

Equation (2.14) implies that the normal component of the electric potential is zero. Fig. 2.6 shows the active boundary conditions in PDE mode.

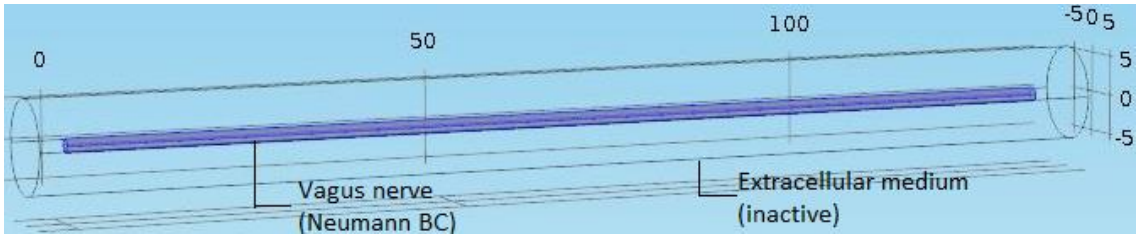

Fig. 2.6. Boundary conditions in the PDE mode. The Vagus nerve with Neumann Boundary conditions is shown in dark blue.

In the electrostatics mode, the boundaries of the vagus nerve are selected as the electric potential sources with coupling variable u_1, whereas all the boundaries of the extracellular sub-domain are set to ground [9]. Mathematically, it can be described as:

$$V = 0 \text{ (at the boundaries of the extracellular sub-domain)} \tag{2.15}$$

$$V = u_1 \text{ (at the boundaries of the vagus nerve).} \tag{2.16}$$

Fig. 2.7 shows the active boundary conditions in Electrostatics mode.

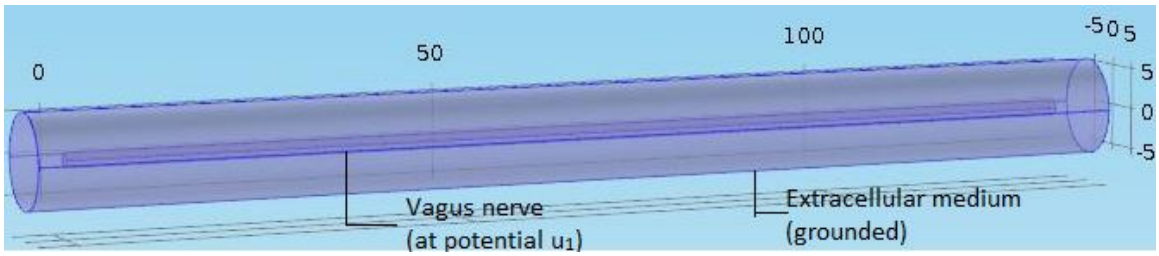

Fig. 2.7. Boundary conditions in the Electrostatics mode. Boundaries are marked in dark blue. The extracellular medium boundaries are grounded whereas the vagus nerve boundaries are set to the actual electric potential u_1.

2.1.6 Meshing

The mesh divides a complex geometry into small units having simple geometrical shapes like tetrahedral, hexahedral, prism etc. These small units are called mesh elements. The benefit of meshing lies in the fact that now the solver just has to solve all these simple mesh elements and combine their solutions instead of solving a complex geometry all at once.

There are two primary meshing techniques: Physics-controlled meshing and user-controlled meshing. The default is to use a physics-controlled mesh. In physics-controlled meshing, the mesh adapts itself to the model's current physics settings. The benefit of using this meshing technique is that whenever there are any changes made in the physics settings of the model, all those changes would be reflected on the mesh setting automatically. The drawback of using physics-controlled meshing technique is that one cannot have different element sizes for individual domains. It has just one element size for the

entire geometry. In a user-controlled mesh, the user is free to use different element sizes for different domains as per his requirement [2].

In this test bed model a user-controlled mesh has been employed with tetrahedral shaped mesh elements. Here the physics is not changing so much that a physics-controlled mesh is needed. More importantly, this test bed model requires having element size finer around the vagus nerve and coarser in the extracellular medium for a reliable and accurate simulation, which is possible only by using a user-controlled mesh. Fig.2.8 shows a cross section of the meshed model.

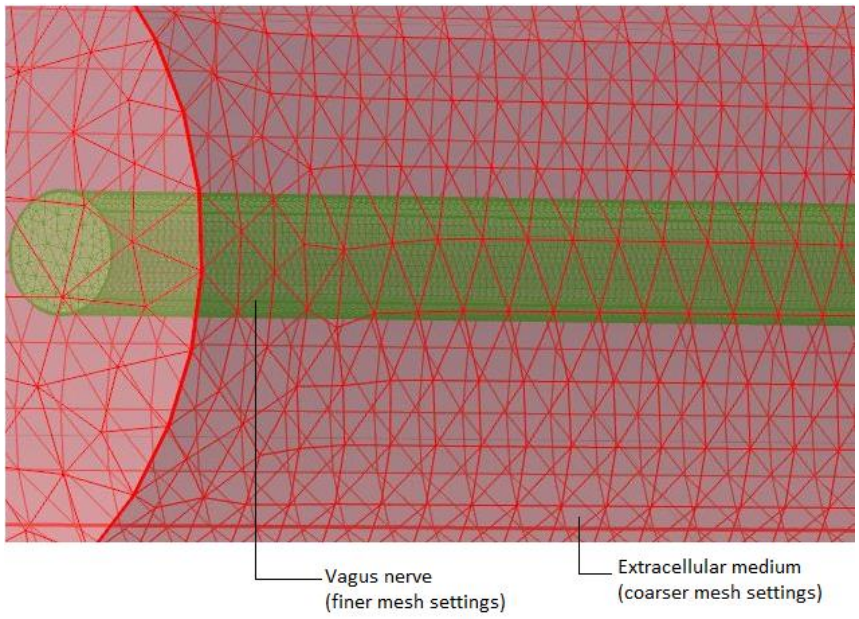

Fig.2.8. Meshed Model (the red mesh is for the extracellular sub-domain (coarser) and the green mesh is for the vagus nerve sub-domain (finer)).

2.1.7 Solver Configuration

Since we are doing a time dependent study of the propagation of action potential through the vagus nerve, a time dependent solver the “Geometric Multigrid” solver is used to carry out the time dependent analysis.

2.1.8 Running the Simulation

Once the vagus nerve geometry was built and the simulation parameters were configured, the final step was to run the simulation. For some complex models, like the one developed here, it is difficult to run the simulation on a standard desktop or a personal laptop computer. The simulations require a lot of memory (RAM) which might not be available in standard standalone machines or personal laptops. To overcome this issue, the Clemson University’s primary high performance computing (HPC) resource, the Palmetto cluster [14] was used.

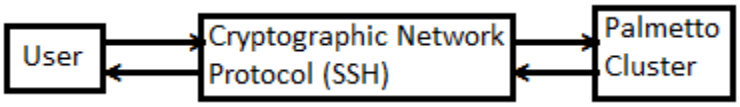

Fig.2.9. Establishing a remote connection to the cluster

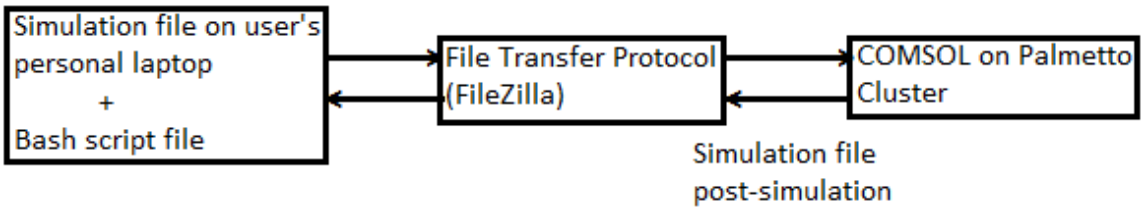

Fig.2.10. Process to submit a simulation file to the cluster

The Palmetto cluster is suitable to run such complex simulation jobs which might otherwise take days to run on a regular standalone machine or a personal laptop (of course if the machine or the laptop doesn't crash before that). Running the simulation job on the Palmetto cluster produces simulation results quickly. One has to develop a bash script consisting of details like the filename of the file that needs to be submitted, the memory that the user wants to allocate on the Palmetto cluster to run the simulation on the submitted file, the maximum time for which the user wants to run the simulation on the submitted file and finally the output filename of the simulated file. Once the file is submitted on the cluster (Fig. 2.10), the user gets an email message confirming the successful file submission. If errors are detected while simulating the model, the simulation is terminated and the user is notified of the incorrect simulation through an email message. The user can then download the file, make the required changes and then re-submit the file on the Palmetto cluster. Finally, once the execution has successfully completed, the user gets an email message that the execution was successful and the simulated file is ready to be

downloaded from the Palmetto cluster. Notice here that the simulated file will have the output filename that the user specified in the bash script.

2.1.9 Test Bed Simulation Results and Discussions

2.1.9.1 Action Potential (AP) Propagation through the Vagus Nerve

The action potential propagation pattern through the length of the vagus nerve at different times can be seen in the figure below (Fig. 2.11).

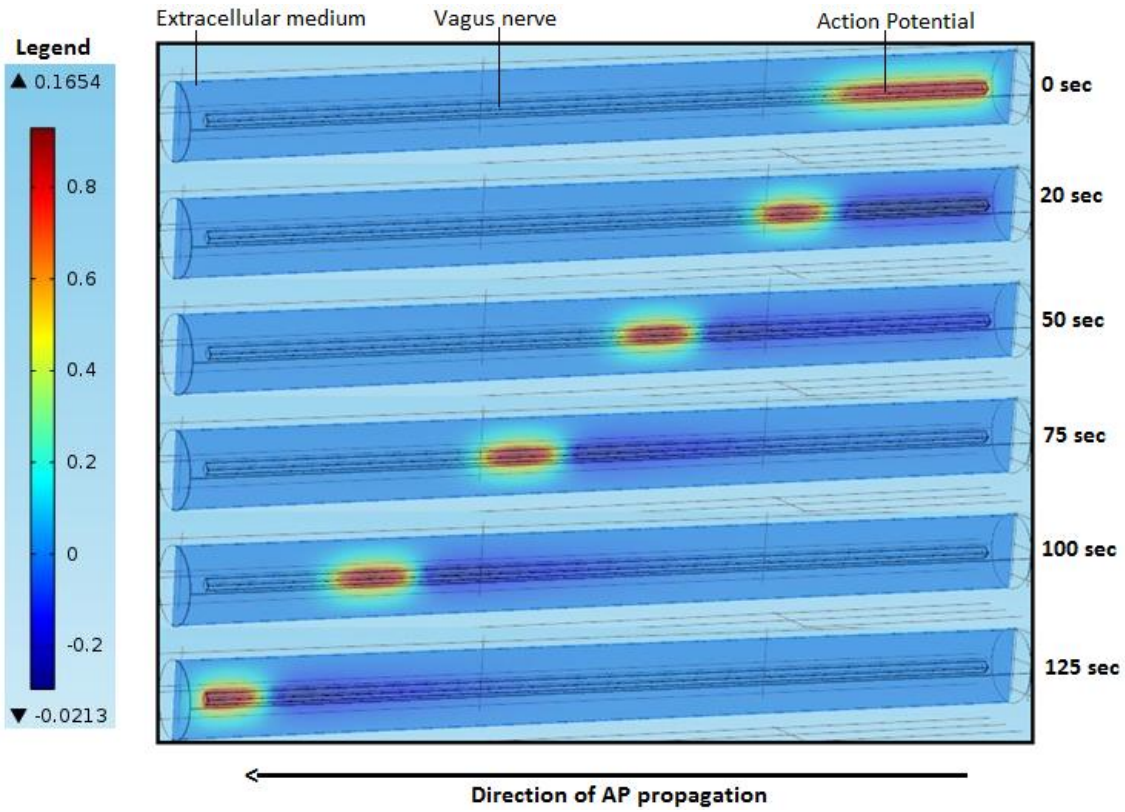

Fig.2.11. AP propagation pattern through the vagus nerve at different times.

2.1.9.2 A Check to Ensure that the Action Potential is Generated by the External Applied Potential

The vagus nerve test bed in this project has been developed using the Fitzhugh-Nagumo equations. Fitzhugh-Nagumo equation based models are such that they support the action potential propagation through the nerve by regenerating it at regular intervals. The first step to validate this model is to make sure that the action potential in the vagus nerve is generated due to the external applied potential and not by the Fitzhugh-Nagumo model itself. This can be done by setting the initial values of u_1 and u_2 to 0. By doing so, the action potential should not be generated in the vagus nerve. If after doing that, there is still an action potential being propagated through the vagus nerve, then that means the Fitzhugh-Nagumo model is itself generating the action potential and the applied potential is not significant to the model. This should not be the case as it would defeat the purpose of external electrical stimulation of the vagus nerve.

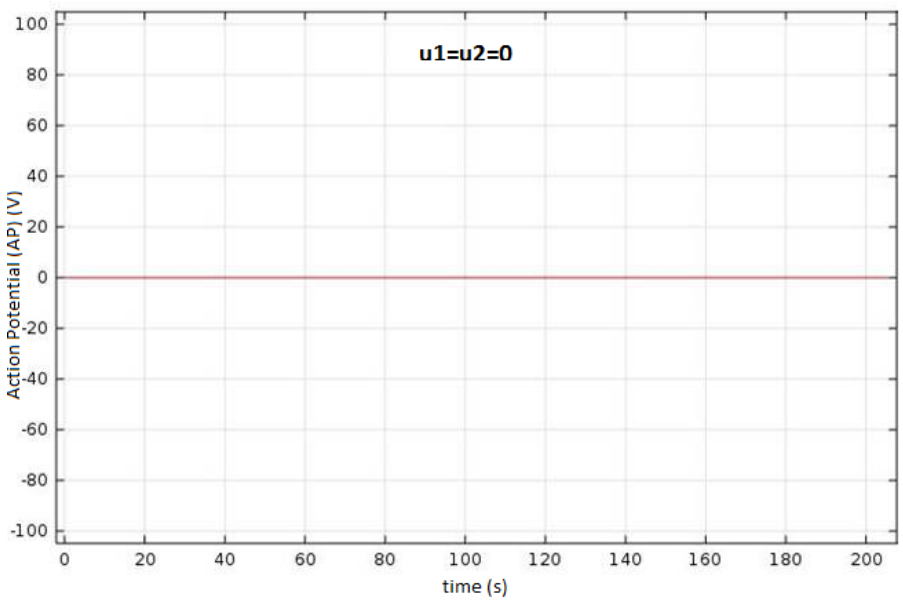

Fig.2.12. AP=0 when u_1=u_2=0.

Fig. 2.12 shows that when the initial values of u_1 and u_2 are set to 0, no action potential propagation is observed through the vagus nerve (AP=0). Hence the claim that action potential is generated only by the applied potential is validated.

2.1.9.3 Action Potential (AP) at the Beginning & at the End of the Vagus Nerve

Inbuilt probes in COMSOL Multiphysics simulation software can be used to monitor the development of action potential at the beginning and at the end of the vagus nerve. There are a number of probes one can make use of in COMSOL Multiphysics like domain probes, boundary probes, edge probes, domain point probes, boundary point probes, global variable probes etc. [1]. For

this application, a boundary probe was the best choice as it provides the action potential values at the starting (Fig. 2.13 a) and the ending boundary of the vagus nerve (Fig. 2.14 a).

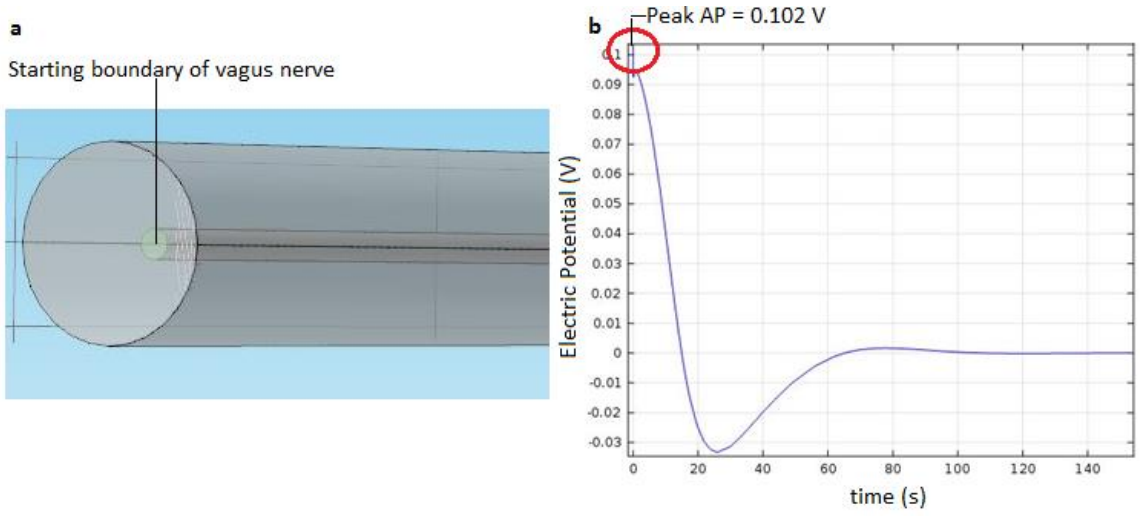

Fig.2.13 (a). A boundary probe monitoring the development of AP at the beginning of the vagus nerve. **(b)** AP on the vagus nerve at that boundary.

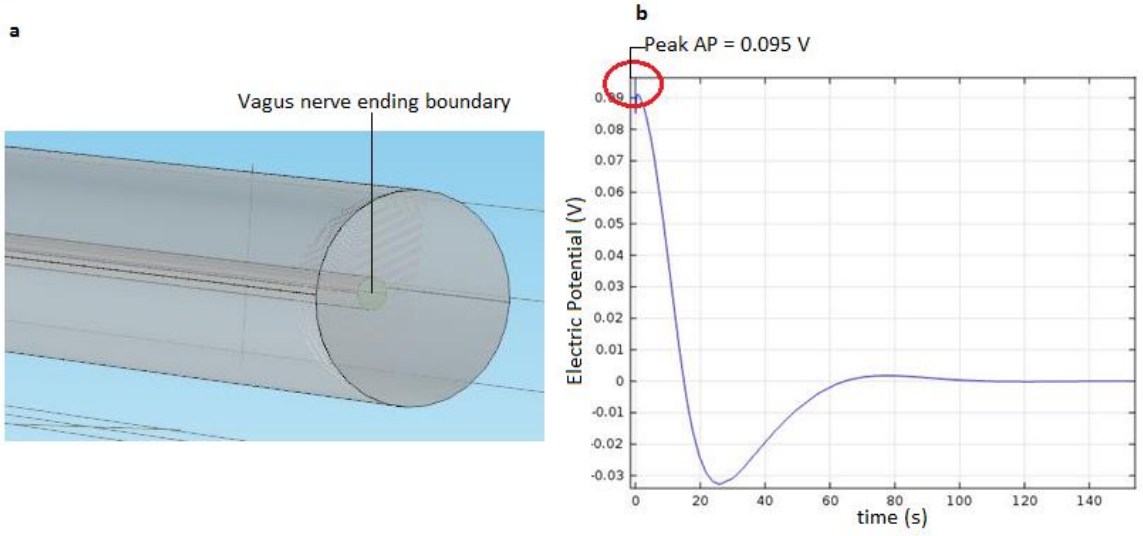

Fig.2.14 (a). A boundary probe monitoring the development of AP at the end of the vagus nerve. **(b)** AP on the vagus nerve at that boundary.

The plots obtained here resemble the characteristics of a typical action potential along any nerve (Fig. 2.13 b, 2.14 b). It can be inferred from the two plots shown above that not only is the action potential is being generated by the applied external potential, it is also being propagated through the entire length of the vagus nerve with almost a constant amplitude. This captures the salient behavior inside a real nerve, i.e. the action potential propagates through the length of the nerve with constant amplitude, and therefore validates this vagus nerve test bed model.

2.1.9.4 Critical Voltage at which the Action Potential (AP) Fires

To further validate the model, the critical voltage at which the action potential fires was determined. The critical voltage/threshold voltage in this model is set by the parameter α or the excitation threshold. Now to test whether this parameter works as it is supposed to i.e. any external potential less than the value of α should not cause the action potential to fire. α=0.1 V for this model. To test the validity of the above argument, 0.05 V and 0.09 V external potentials were applied to the vagus nerve model via copper electrodes. The system did not execute for both these external potential values and returned an error stating, “Failed to evaluate expression”. But when external potentials having magnitudes 0.1 V or greater were applied, the action potential fired and propagated through the length of the vagus nerve thereby validating the above argument (Fig. 2.15).

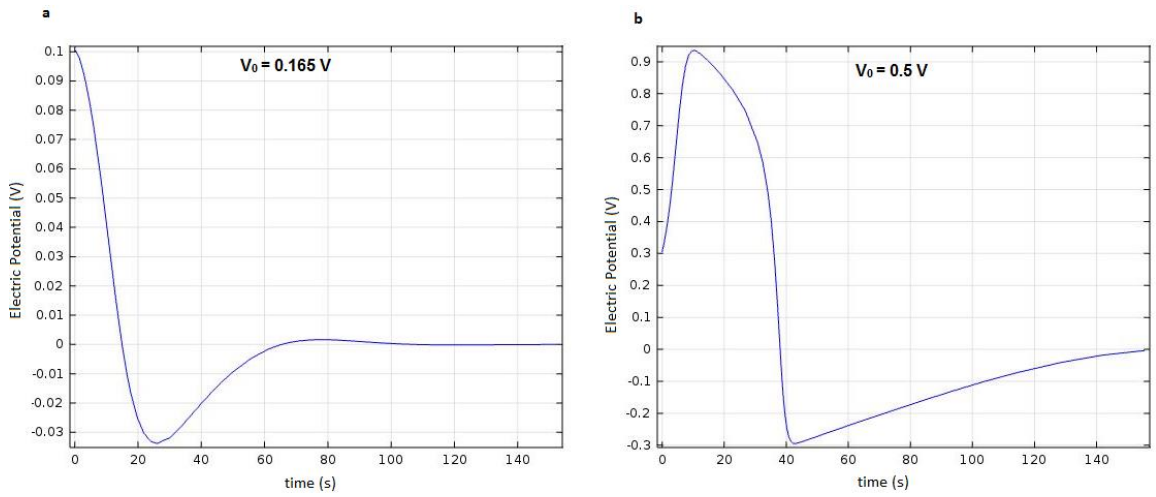

Fig.2.15. AP firing for $V_0 \geq 0.1\,V$.

Therefore, for $\alpha = 0.1\,V$,

External applied potential, $V_0 < 0.1\,V$ → AP does not fire

External applied potential, $V_0 \geq 0.1\,V$ → AP fires.

2.2 Trace Signal Design

As discussed in Chapter 1, the action potential in a human vagus nerve has an amplitude of 100 mV, a duration of about 1 ms and a frequency ranging between 3 Hz – 30 Hz [16, 17]. These parameters form the design parameters that our tracer should satisfy to successfully generate action potential in the vagus nerve. The vagus nerve test bed, developed in the previous section, was used to design the tracer. For the design of the tracer pulse, the following approach was followed. The duration of the pulse was kept fixed at 1 ms, and the

amplitude of the pulse was varied to get the action potential peak amplitude of 100 mV. To vary the amplitude of applied potential on the vagus nerve test bed, the parameter V_0 is changed.

When the tracer having amplitude V_0 = 0.1 V was applied to the vagus nerve test bed, an action potential having peak amplitude of 0.06 V was generated (Fig. 2.16) which was way less than the required action potential peak amplitude of 0.1 V and hence was rejected.

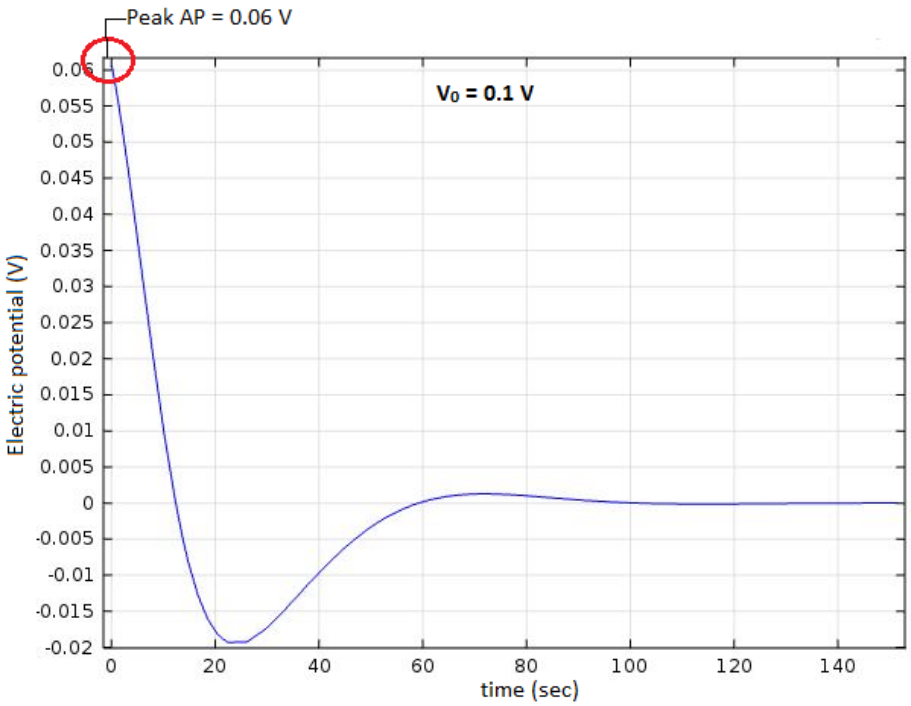

Fig. 2.16. AP plot for V_0 = 0.1V

Then we increased the tracer amplitude to V_0 = 0.15 V and applied this elevated potential value to the vagus nerve test bed. With this value, an action potential having peak amplitude of 0.09 V was generated (Fig. 2.17). It

again fell a little short from the required action potential peak of 0.1 V and hence was rejected as well.

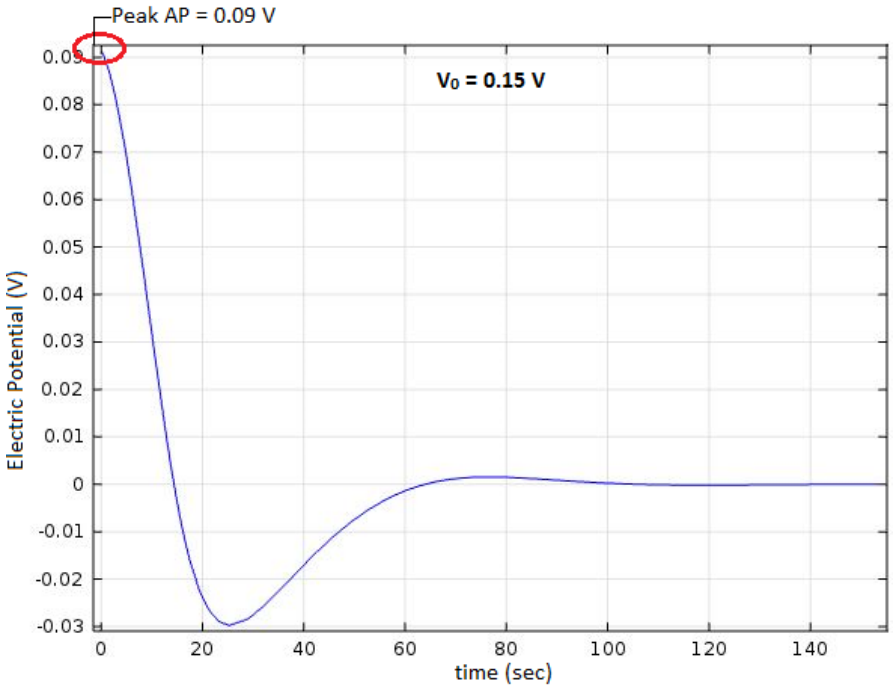

Fig. 2.17. AP plot for V_0 = 0.15V

Then we further increased the tracer amplitude to V_0 = 0.165 V and applied this elevated potential value to the vagus nerve test bed. With this value, we got the required action potential having peak amplitude of 0.1 V (Fig. 2.18) was achieved. This satisfied our design requirement and hence was accepted as the tracer amplitude value.

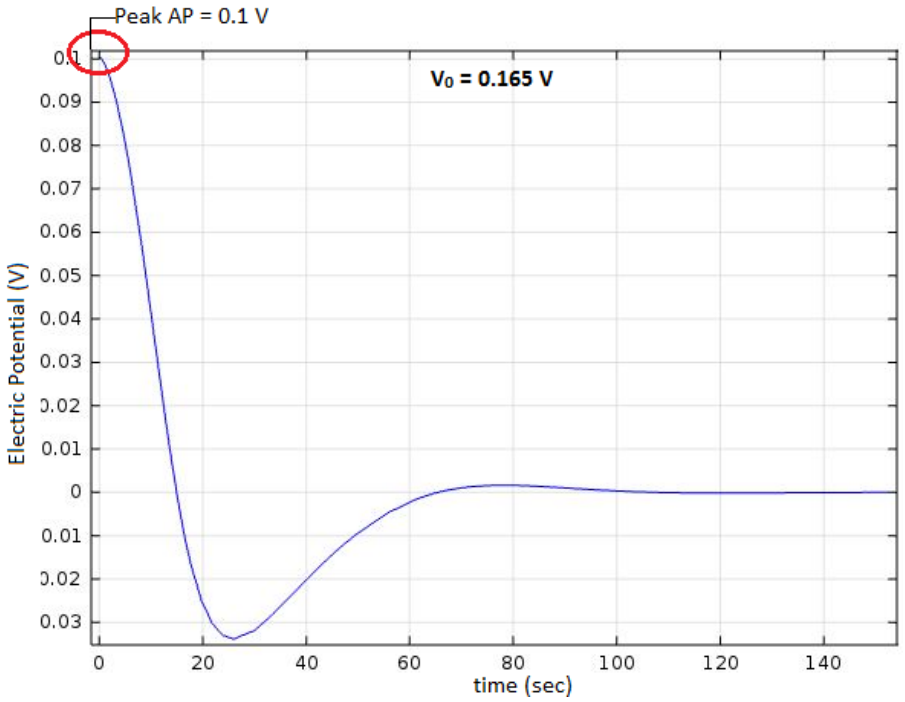

Fig. 2.18. AP plot for V_0 = 0.165V

The tracer pulse was designed using the above design parameters (Fig. 2.19 (a)). Frequency of 30 Hz was selected to design the tracer pulse train (Fig. 2.19 (b)) to decrease the response time of the nerve. At higher frequencies, the nerve gives an immediate firing of action potential under normal circumstances i.e. when no neuromuscular block has been used.

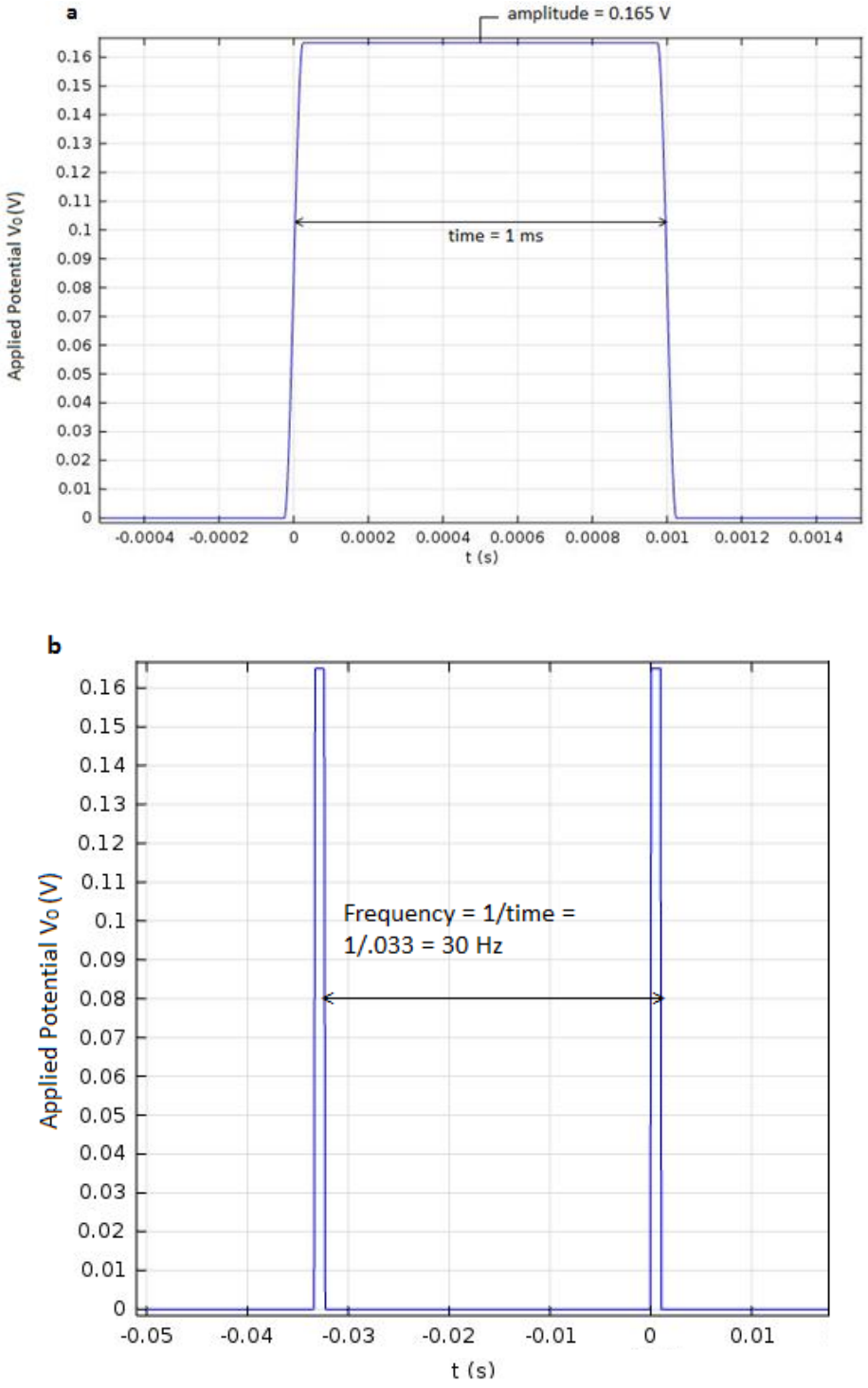

Fig. 2.19 (a). Voltage Pulse to initiate the action potential generation in the vagus nerve test bed.

(b) Voltage pulse train @ 30 Hz.

2.3 Tracer Excitation Cuff Design

For selective activation of the vagus nerve, the tracer excitation electrodes should be placed very close to the nerve. Selective activation improves due to the electric potential gradient which increases as the spacing between the tracer excitation electrode and the vagus nerve is reduced. To get such a selective activation of the vagus nerve, cuff-shaped electrodes would be a likely choice as once these are positioned on the vagus nerve trunk, they are less likely to shift their position relative to the vagus nerve. In addition to selective activation, such a close placement of stimulating electrodes around the vagus nerve can reduce the power requirement demand of the stimulator as very little power would be needed to conduct through the small space between the stimulating electrode and the nerve [10].

The tracer excitation cuff should be able to deliver the excitation trace V_0 (designed in the previous section) to the vagus nerve, to generate an action potential in the vagus nerve. The vagus nerve simulation test bed was used to refine the parameters of the cuff design. To reduce the simulation times, a small section of the vagus nerve test bed is selected for stimulation. Two types of cuff geometries are studied here: (1) full cuff and (2) half cuff geometry. The distance between the two tracer cuffs is 1 cm and is kept the same for both the geometries. The design procedure involves stimulating the vagus nerve test bed

section using both the cuff geometries and finalizing the tracer cuff geometry that can deliver the right V_0 to the vagus nerve test bench.

2.3.1 Geometry

In COMSOL multiphysics, the tracer excitation full cuffs are modeled as hollow cylinders having diameter 2 mm, width 1 mm and thickness 250 µm (Fig 2.20 (a)). The tracer excitation half cuffs, on the other hand, are modeled with the same parameters but with half of their boundary surfaces removed (Fig 2.20 (b)). The separation between the two cuffs in both the cases is taken as 1 cm. These electrode parameters are commonly used for different nerve stimulations including Vagal Nerve Stimulation (VNS) [8, 9]. Neither the full cuffs nor the half cuffs physically touch the vagus nerve model to avoid any damage to the nerve.

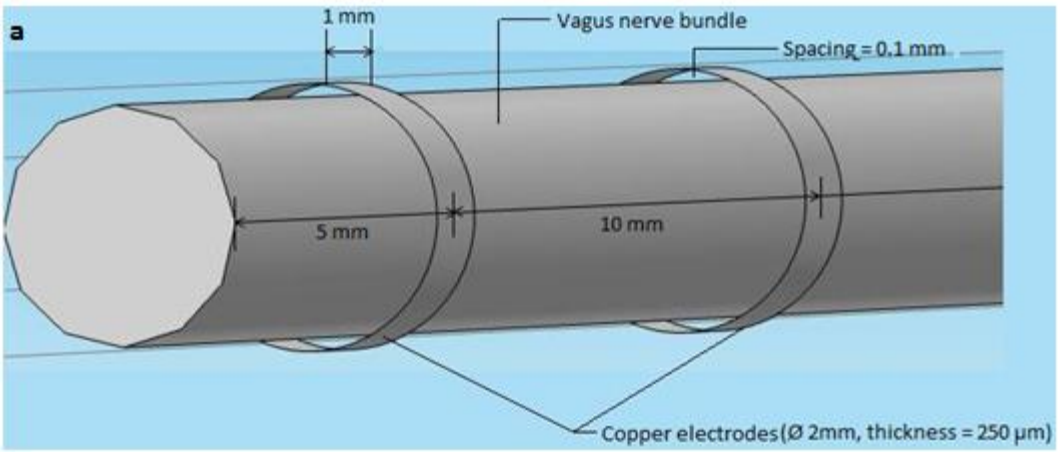

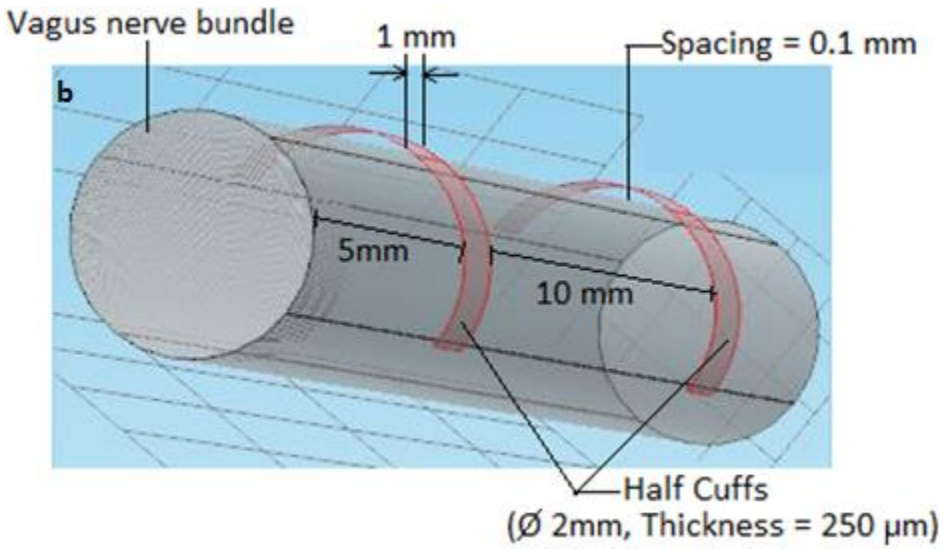

Fig. 2.20 (a). Tracer excitation full cuff geometry , **(b)** Tracer excitation half cuff geometry.

The superpositioning of the two cylinders, depicting the vagus nerve and the extracellular medium, result in the gap between the tracer excitation cuffs and the vagus nerve bundle being filled with extracellular media for both the cuff geometries (Fig. 2.21).

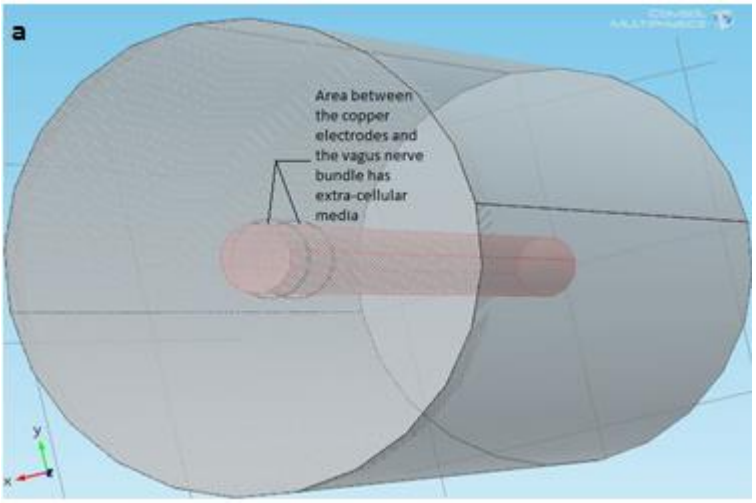

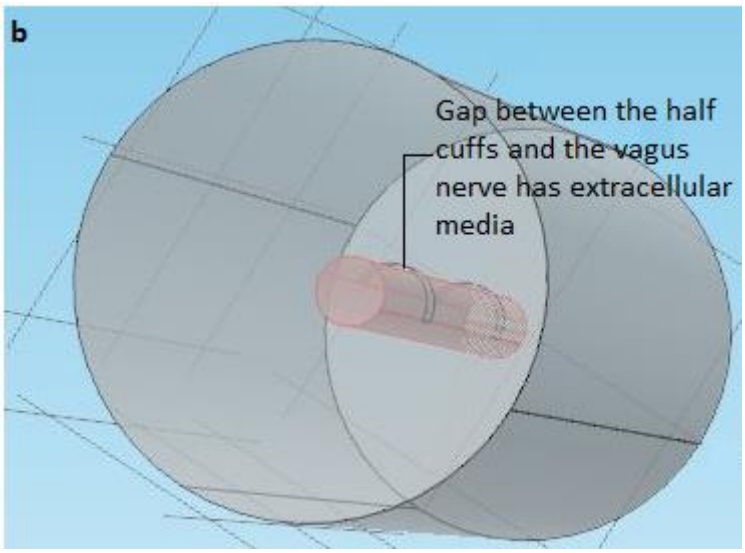

Fig. 2.21. (a) Gap between the tracer excitation full cuffs and the vagus nerve bundle has extracellular media, **(b)** Gap between the tracer excitation half cuffs and the vagus nerve bundle has extracellular media

2.3.2 Material

Copper is used to design both of the tracer excitation cuff geometries (full cuff and half cuff). Copper is predefined in COMSOL's material library and can be used directly in this design without the need to specify any material properties. The predefined material properties for Copper (Cu) used to build the electrodes are presented in Table 2.4.

PROPERTY	NAME	VALUE	UNIT
Relative permeability	mur	1	1
Electrical conductivity	sigma	5.998e7	S/m
Heat capacity at constant pressure	Cp	385	J/(kg.K)
Relative permittivity	epsilonr	1	1
Surface emissivity	epsilon_rad	0.5	1
Density	rho	8700	kg/m^3
Thermal conductivity	k	400	W/(m.K)
Reference resistivity	rho0	1.72e-8	Ω.m
Resistivity temperature coefficient	alpha	3.9e-3	1/K
Reference temperature	Tref	273.15	K

Table 2.4. Predefined Copper Material Contents [2].

2.3.3 Subdomain Settings and Boundary Conditions

Here, the electrostatics physics interface is employed for the entire system, which is found under the AC/DC branch. In the case of the full cuff geometry, the subdomain settings are such that tracer excitation full cuffs are the sub-domain. In the case of the half cuff geometry, the subdomain settings are such that tracer excitation half cuffs are the sub-domain. In both the cases, V is the dependent variable. The electrostatic mode solves equations (2.10) and (2.11). The initial value of the dependent variable being solved for here, V is taken to be V_0 i.e. the above designed tracer having amplitude V_0 is applied to one cuff and the other cuff is grounded. The initial electric potential values of the vagus nerve and the extracellular medium are set to zero (Fig. 2.22).

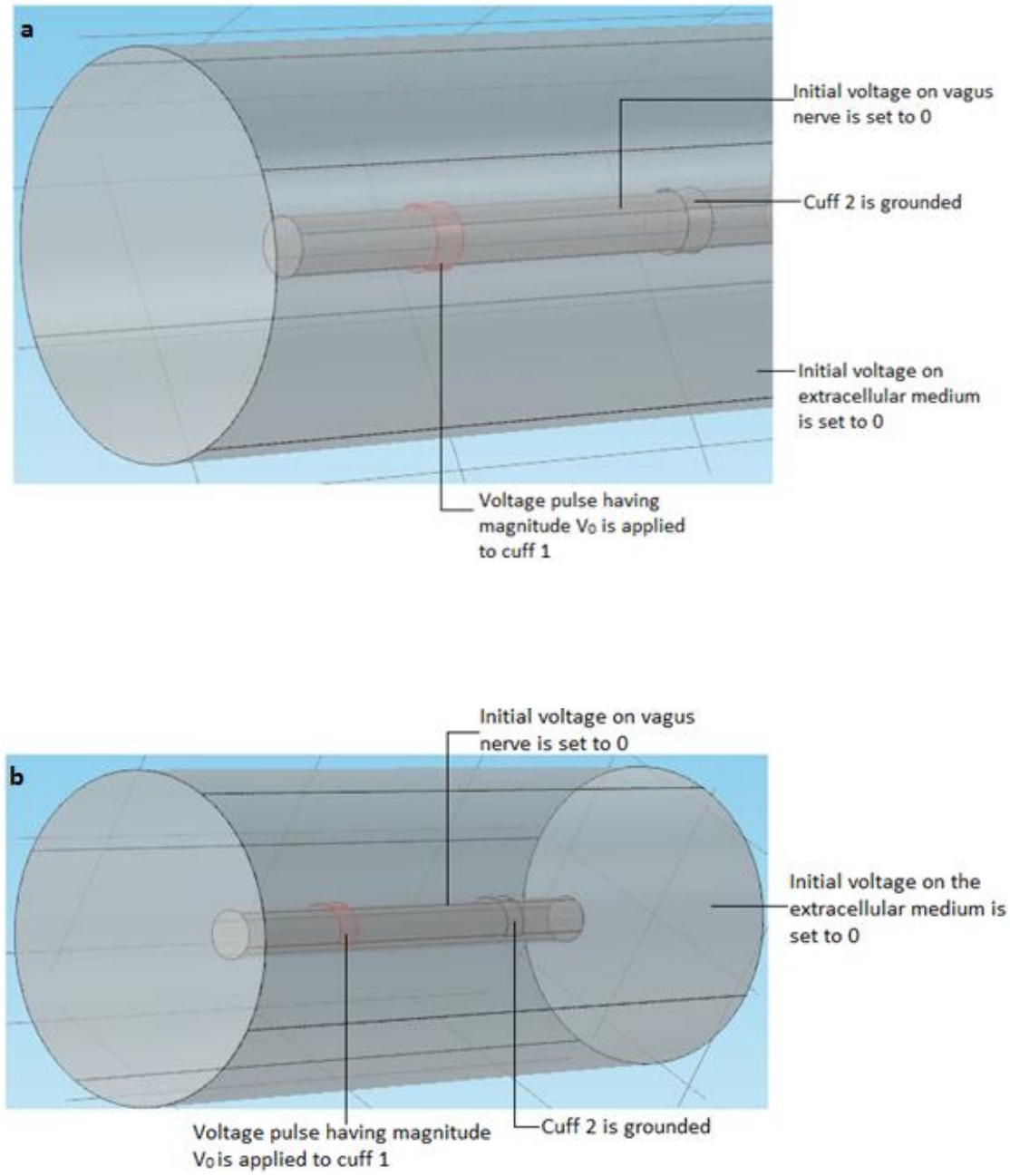

Fig. 2.22. (a) Sub-domain settings and boundary conditions for **(a)** tracer excitation full cuffs and **(b)** tracer excitation half cuffs.

2.3.4 Meshing

A user-controlled mesh has been employed with tetrahedral shaped mesh elements. Here, the physics is not changing so much that a physics-controlled mesh is needed. More importantly, this design requires having very fine mesh elements around the tracer excitation full and half cuffs, a little coarser mesh elements for the vagus nerve, and coarse mesh elements for the extracellular medium for a reliable and accurate simulation, which is possible only by using a user-controlled mesh. Fig. 23 shows a cross section of the meshed design.

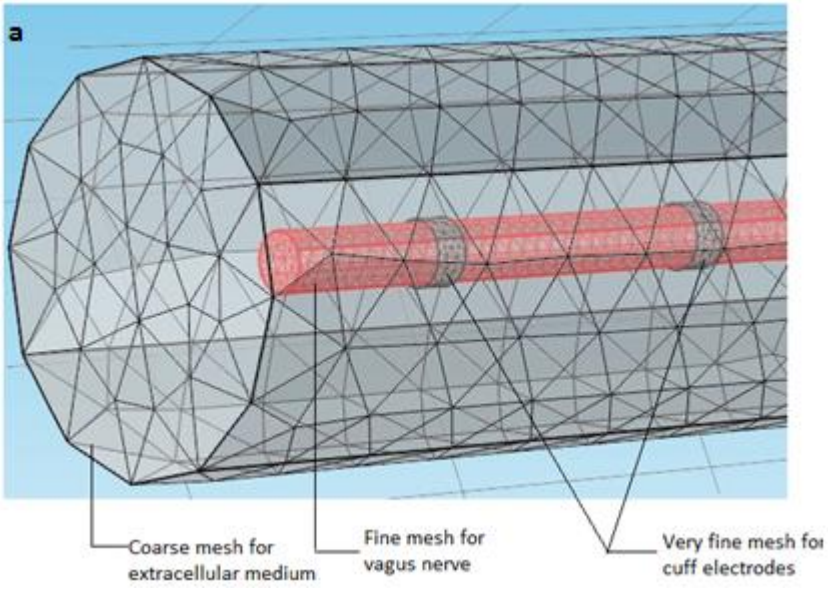

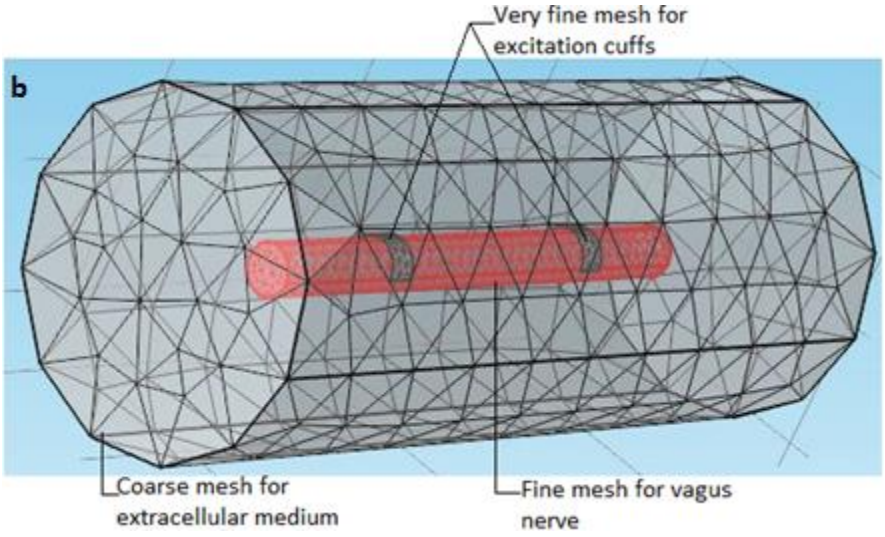

Fig. 2.23. Meshed design for **(a)** full cuff and **(b)** half cuff geometries.

2.3.5 Solver Configuration

To simulate the tracer excitation full cuffs and half cuffs design, a stationary study of the voltage pulse transmitted through the electrode to the vagus nerve is done. Therefore, to solve this system a stationary solver is employed.

2.3.6 Running the Simulation

The simulation of the tracer excitation full cuffs and half cuffs design is not computationally heavy since it is a stationary study, a personal laptop with standard RAM configuration was used for this simulation.

2.3.7 Designed Tracer Applied via Tracer Excitation Full Cuffs and Half cuffs to the Vagus Nerve Test Bed

Fig. 2.24 (a) and (b) show the simulation of the application of the designed tracer signal to the vagus nerve test bed through the tracer excitation full and half cuffs respectively.

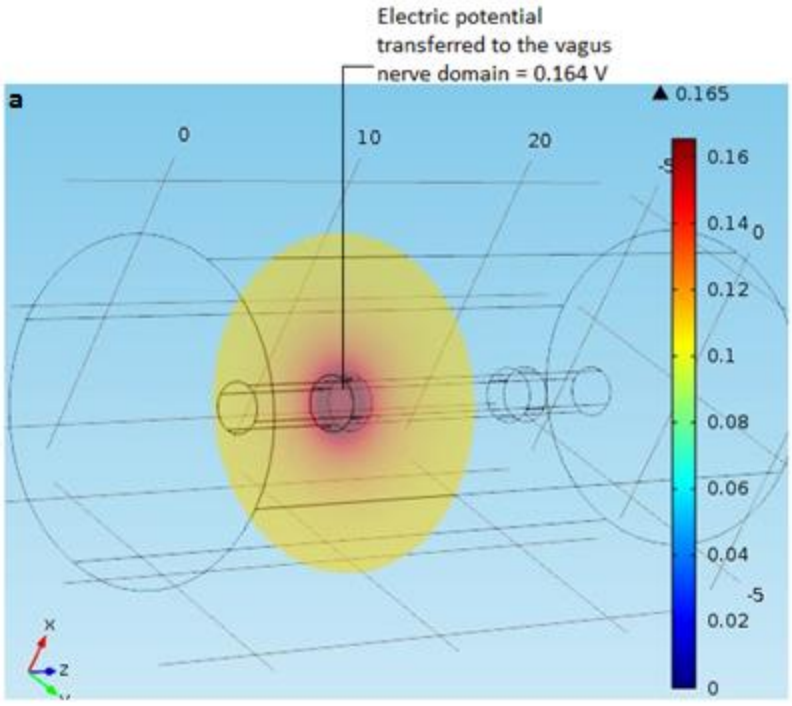

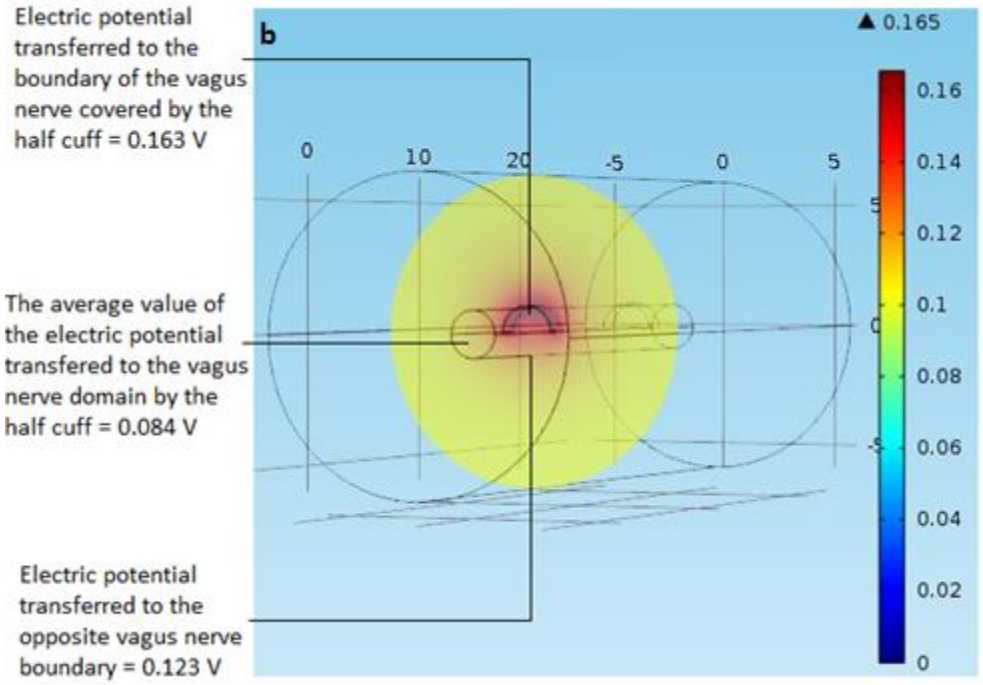

Fig.2.24. Application of the designed tracer to the vagus nerve test bed **(a)** through tracer excitation full cuffs and **(b)** through tracer excitation half cuffs.

As seen from Fig. 2.24(a), the tracer excitation full cuffs transfer the entire tracer to the vagus nerve test bed and this tracer should be able to artificially depolarize the transmembrane potential beyond its threshold and thus induce an action potential in the vagus nerve. Whereas, the tracer excitation half cuffs transfer do not transfer the entire tracer to the vagus nerve test bed (Fig. 2.24 (b)). The average value of the potential that is induced in the vagus nerve test bench is almost 50% less than what is applied to the excitation cuff. Therefore, this tracer would require a larger input voltage in order to induce an action potential in the vagus nerve. Another observation that can be made from Fig 2.24 is that the spread of tracer transferred by the full cuffs is radially

symmetric whereas the spread of the tracer transferred by the half cuffs is not. This further reduces the potential for half-cuff to induce a propagating action potential.

From the results shown above, the tracer excitation full cuffs are recommended over the tracer excitation half cuffs. There is one scenario where the tracer excitation half cuffs may be preferred over the tracer excitation full cuffs and that is during a laparoscopic vagotomy where it may be too difficult to attach the full cuffs. In this case, to transfer the designed tracer to the vagus nerve, an electric potential having double the amplitude value than the designed tracer should be applied to the tracer excitation half cuffs (in this case 0.33 V). On simulating the half cuff design with this value, it was observed that the average value of the potential that is transferred to the vagus nerve test bench came out to be very close to the designed tracer value (Fig. 2.25). This signal can therefore artificially depolarize the transmembrane potential beyond its threshold and thus induce an action potential in the vagus nerve.

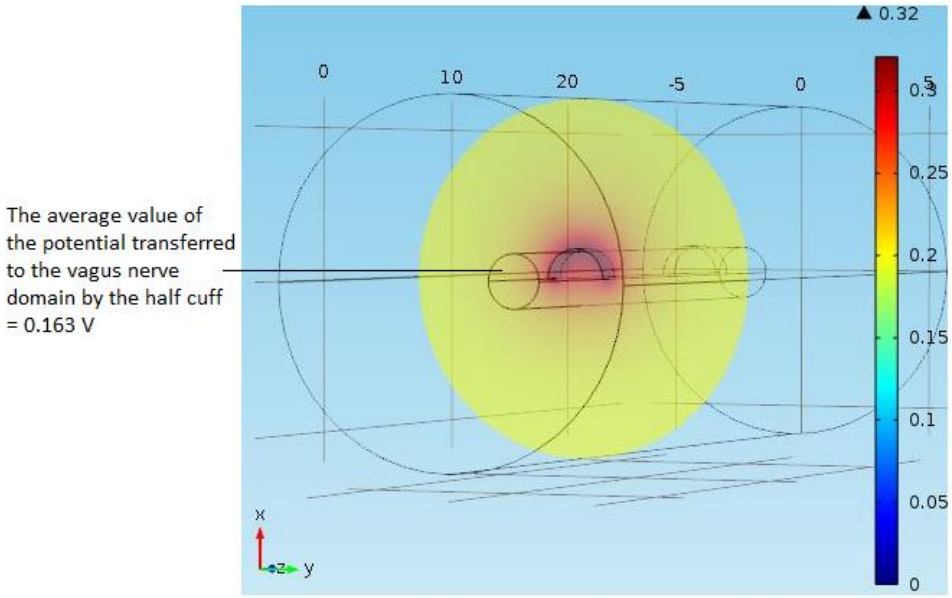

Fig.2.25. Application of an electric potential value twice the designed tracer value through tracer excitation half cuffs and to induce AP in the vagus nerve.

References

[1] R. Appali, S. Petersen, J. Gimsa and U.V. Rienen, “3D-Simulation of Action Potential Propagation in a Squid Giant Axon, Proceedings of the COMSOL Conference (2009).

[2] COMSOL Multiphysics User’s Guide, Version 4.3.

[3] A.L. Hodgkin and A.F. Huxley, “A quantitative description of membrane current and its application to conduction and excitation in nerve”, Journal of Physiology, vol. 117, pp. 500-544 (1952).

[4] C. Koch, Biophysics of computation: information processing in single neurons, Ney York, NY [u.a.], Oxford Univ. Press, (1999).

[5] Y.P. Guo, J.G. McLeod and J. Baverstock, “Pathological changes in the vagus nerve in diabetes and chronic alcoholism”, Journal of Neurology, Neurosurgery, and Psychiatry, 50:1449-1453, 1987.

[6] “Transvascular nerve stimulation apparatus and methods”, http://www.google.com/patents/US8571662, last accessed 06/19/2014.

[7] Baccaro et al., Anat Physiol, 2013.

[8] VNS Therapy System Physician’s Manual, May 2014.

[9] “Nerve Cuff Electrodes”, http://www.microprobes.com/index.php/products/emg-patch-electrodes/nerve-cuff-electrodes, last accessed 06/19/2014.

[10] J.T. Mortimer and N. Bhadra, “Peripheral Nerve and Muscle Stimulation”, http://cwru.edu/groups/ANCL/pages/99/Ch4-2-Preprint.pdf, last accessed 06/24/2014.

[11] R. Szmurlo, J. Starzynski and S. Wincenciak, “Numerical model of vagus nerve electrical stimulation”, COMPEL Vol. 28 No.1, pp. 211-220, 2009.

[12] T. Heimburg, “The Capacitance and Electromechanical Coupling of Lipid Membranes Close to Transitions: The Effect of Electrostriction”, Biophysics Journal, Vol. 103, pp. 918-929, September 2012.

[13] R. Appali, S. Petersen, J.Gimsa and U.V. Rienen, “3D-Simulation of Action Potential Propagation in a Squid Giant Axon”, COMSOL Conference Proceedings, 2009.

[14] “Palmetto Cluster”, http://citi.clemson.edu/palmetto/, last accessed 06/19/2014.

[15] S. Karamcheti and J. Kravitz, “Analyzing Cardiac Action Potentials with the Fitzhugh-Nagumo Model”, http://cosmos.ucdavis.edu/archives/2012/cluster9/kravitz_joshua.pdf, last accessed 07/20/2014.

[16] E.R. Kandel, J.H. Schwartz, and T.M. Jessell, Principles of Neural Science, McGraw-Hill (2000).

[17] P.Boon, I. Moors, V. D. Herdt, and K. Vonck, “Vagus nerve stimulation and cognition”, Seizure Vol 15, June 2006.

CHAPTER 3

TRACER DETECTOR DESIGN

3.1 Need for a Tracer Detector

The overall motivation behind this project was to design a system that would enable the surgeons overcome the major complication of vagotomy surgery, i.e. locating the branches of the vagus nerve. The first part of the system is a stimulating cuff electrode, the design was shown in the previous chapter. The cuff electrodes inject the electronic trace signal into the nerve at a point close to the stomach, a point that is clearly visible and easily accessible. The electronic trace signal is in the form of an electric potential, having amplitude greater than the threshold level, which when applied leads to the generation of action potential that propagates through the length of the nerve.

The second part of the system is a trace detector to indicate the presence of the action potential in a vagus nerve branch. This would enable the surgeon to identify and cut the correct vagus nerve branch and ensure the success of the surgery. Thus there is a need to design a trace detector that would facilitate detection of the action potential propagating through the length of the vagus nerve. Two possibilities were considered, the trace detector could be mounted to a laparoscopy tool as its tip (Fig. 3.1) or the native end effector of the laparoscopy tool itself could be used as the trace detector. A number of trace

detector candidates were considered in order to provide maximum sensitivity and robustness to position and orientation relative to the nerve. The candidate detector probes were modeled in COMSOL Multiphysics 4.3b simulation software.

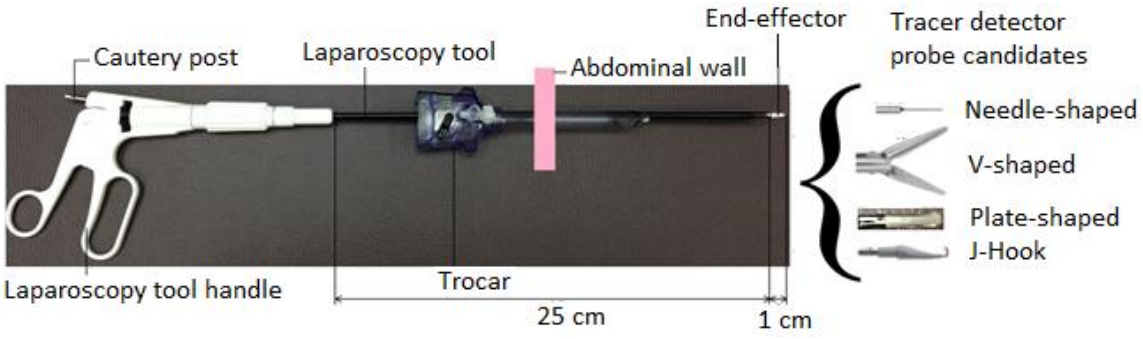

Fig.3.1. Mechanical considerations of the tracer detector system [1].

The laparoscopy tool shown in Fig. 3.1 illustrates mechanical considerations constraining the detector probe design. The embodiment of the tracer detector design pursued in this work is that of a laparoscopy tool with the native end effector. In this project, the end effector on the laparoscopy tool with a cautery post on the tool handle is used to provide an electrical connection from outside the body for the trace detector.

3.2 Tracer Detector Probe Design

Different kinds of tracer detector probe candidate shapes (Fig. 3.1), viz. needle-shaped, plate-shaped, v-shaped and j-hook, are studied to be used

with a laparoscopy tool for the purpose of detection of the action potential trace signal propagating through the vagus nerve. From those candidates, one trace detector probe shape was selected based on the following criteria:

i. probe should not damage the nerve;
ii. probe should maximize detection of the trace signal.

The shape of the trace detector determines whether the probe will damage the nerve or not. The sensitivity of the detector probes to the electric field around the vagus nerve is tested by simulation in COMSOL Multiphysics.

3.2.1 Damage to the Nerve due to Shape of the Trace Detector Candidate

If a surgeon makes use of a trace detector that has sharp edges or a trace detector that presses on to the nerve to locate the trace on the vagus nerve branch to cut during a vagotomy surgery, there is a possibility that it can cause damage to the nerve. From the list of potential trace detector candidates, the needle-shaped tracer detector and the v-shaped tracer detector have sharp edges and hence may cause damage the vagus nerve branch while probing during trace detection. However, the j-hook trace detector does not have sharp edges, it has a round surface which reduces the possibility of nerve damage during the detection procedure.

3.2.2 Robustness of the Trace Detector Candidate towards Trace Detection

To study the sensitivity of the trace detector probe candidates, COMSOL Multiphysics simulations were done using the electrostatics physics interface, found under AC/DC module. It was a stationary study type and stationary solvers were used to solve it. In these simulations, a small section of the vagus nerve test bed that was developed in the previous chapter was used (Fig. 3.2).

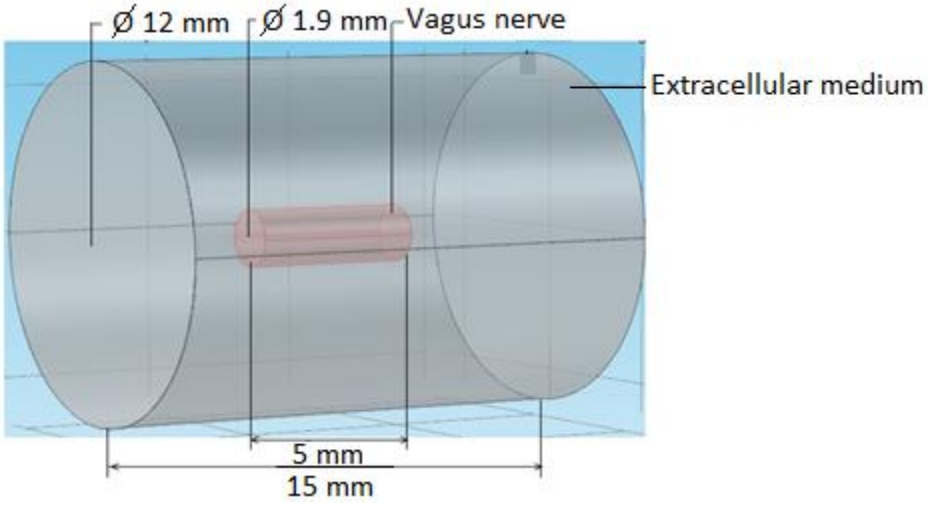

Fig.3.2. Vagus nerve test bed section used in detector probe study.

The different tracer prober candidates were positioned close to the vagus nerve, but did not touch the vagus nerve. The final geometries are shown in Fig. 3.3.

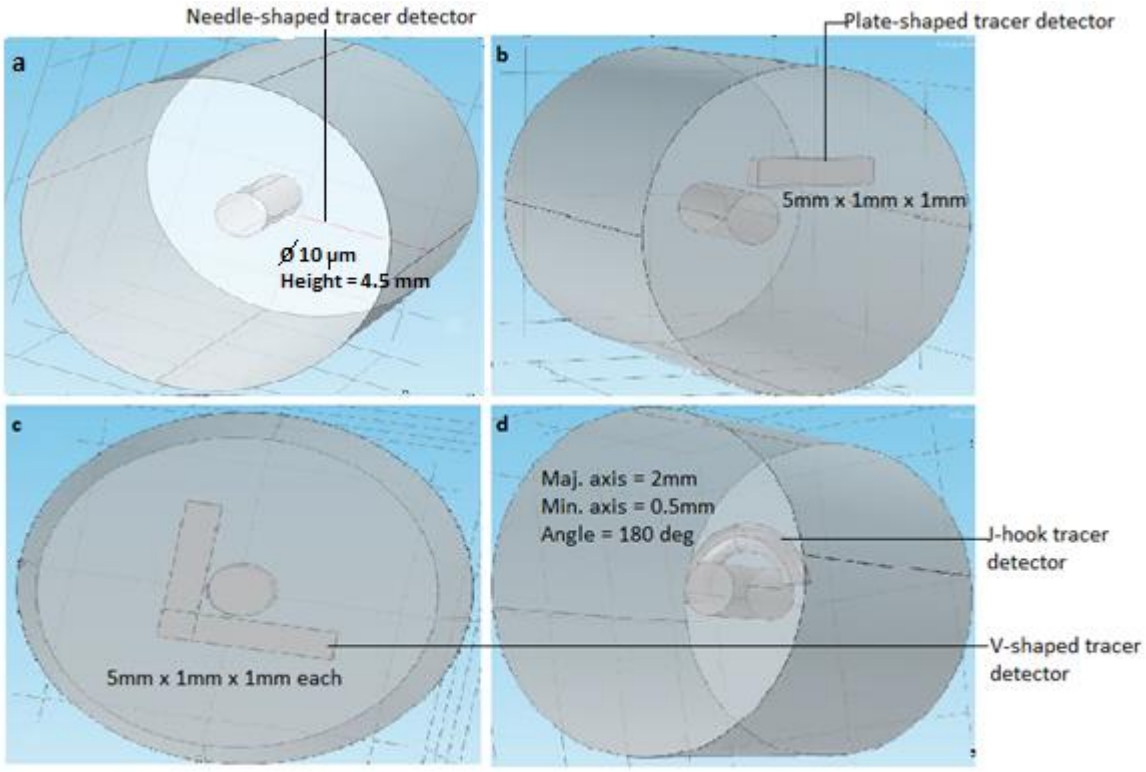

Fig.3.3. Tracer detector geometries and positioning near the vagus nerve **(a)** Needle-shaped tracer detector**, (b)** Plate-shaped tracer detector, **(c)** V-shaped tracer detector, and **(d)** J-hook tracer detector.

A tracer signal in the form of an electric potential having magnitude 100 mV was applied to the vagus nerve and simulation studies to determine the sensitivity of the different tracer detector candidates. The simulation results are shown in Fig. 3.4 – Fig. 3.7.

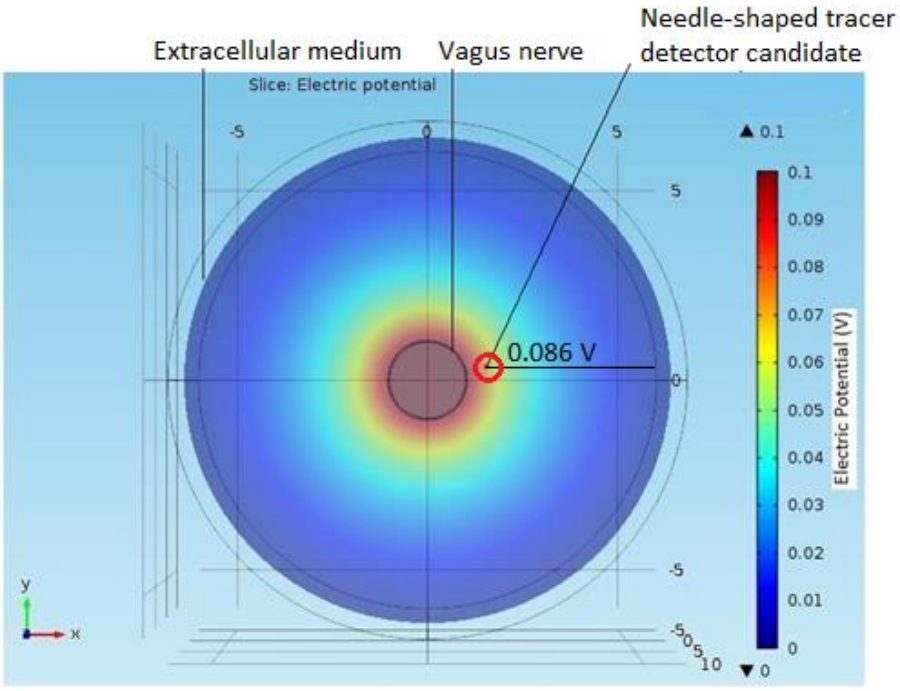

Fig.3.4. Simulation result for needle-shaped tracer detector candidate (view along axis of vagus nerve).

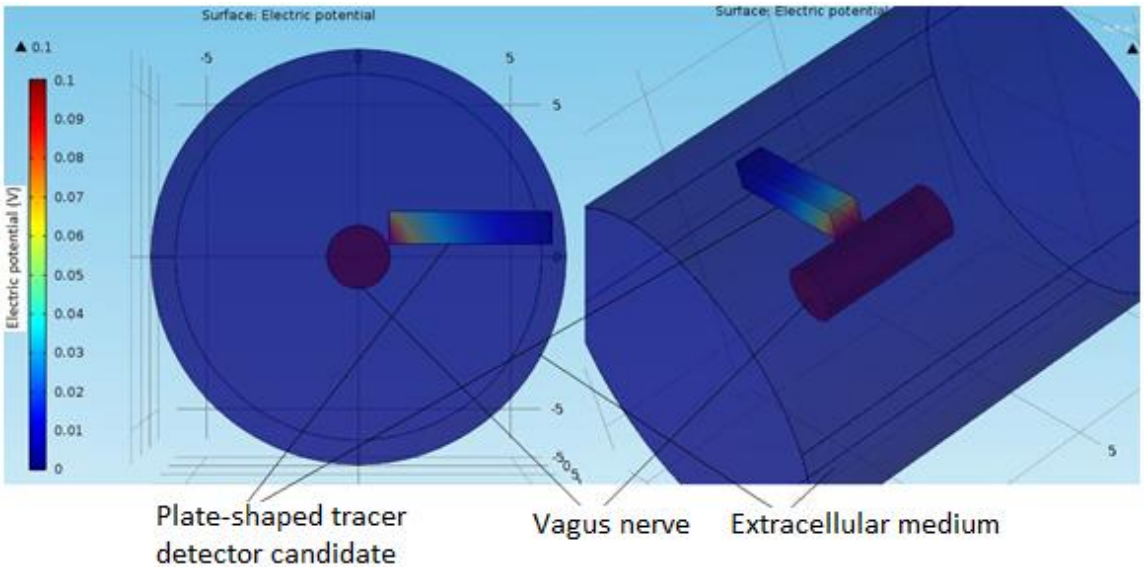

Fig.3.5. Simulation result for plate-shaped tracer detector candidate (view along axis of vagus nerve and 45^{o} off-axis).

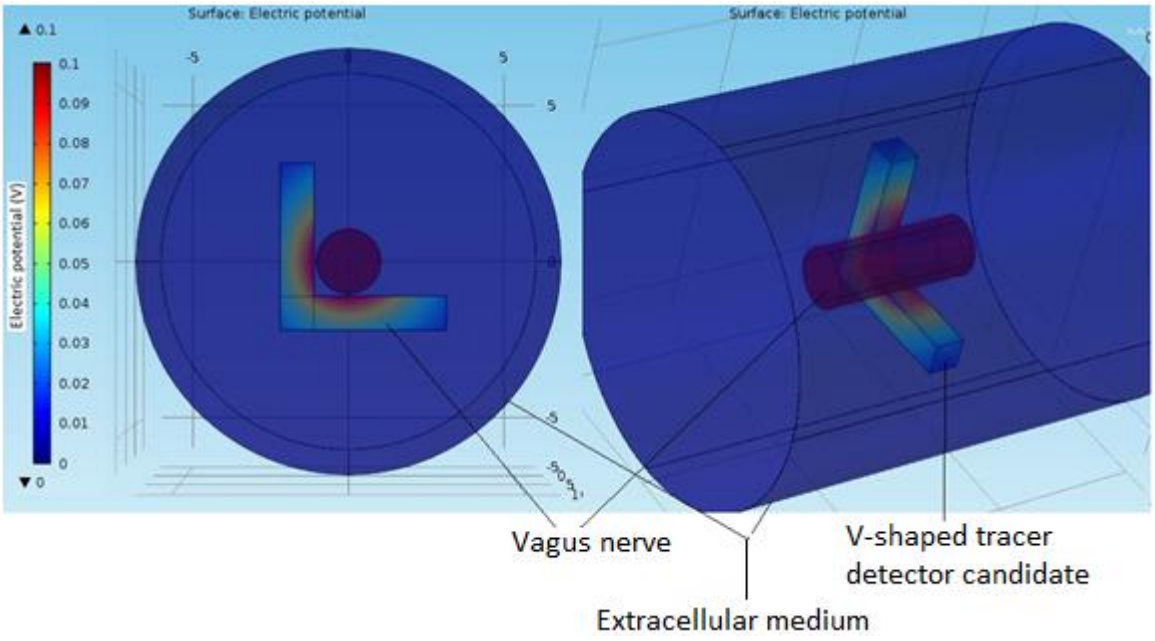

Fig.3.6. Simulation result for v-shaped tracer detector candidate (view along axis of vagus nerve and 45^{o} off-axis).

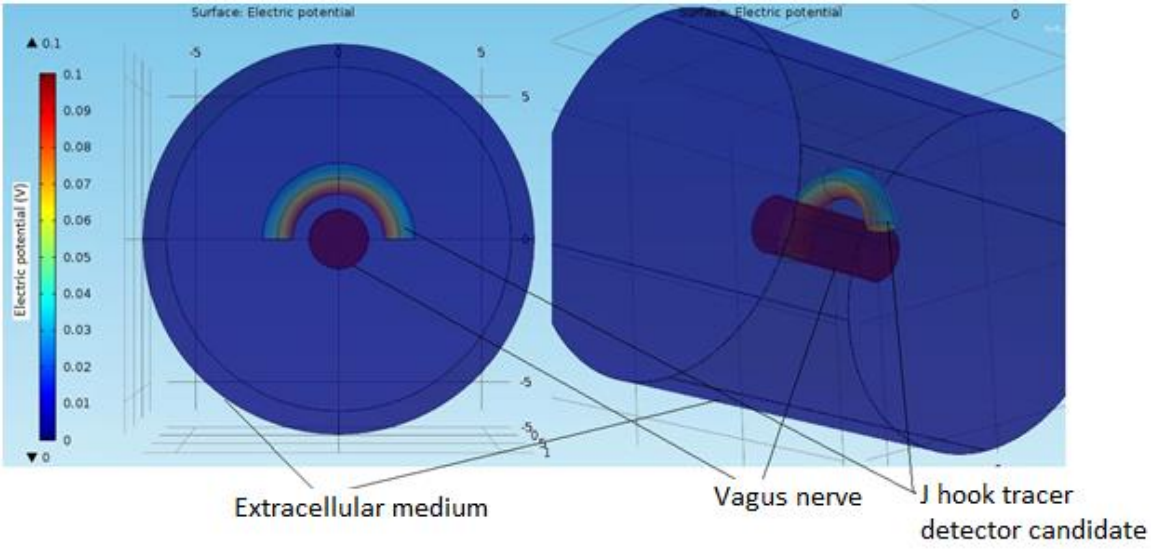

Fig.3.7. Simulation result for j-hook tracer detector candidate (view along axis of vagus nerve and -45^{o} off-axis).

As seen from the simulation results, the needle-shaped tracer detector candidate detects the value of the electric potential trace at its tip (Fig. 3.4). As the needle probe is moved away from the nerve, the measured potential will directly fall off as a function of distance. Similarly, the plate-shaped tracer detector candidate detects the value of the electric potential trace at its edge (Fig. 3.5) and will also be sensitive to minor motion of the probe. Therefore, the robustness of these two tracer detector candidates towards detection of the tracer propagating through the vagus nerve is low since it is a very small surface that detects the value of electric potential trace. In the case of the v-shaped tracer detector candidate, the surface that detects the maximum value of the electric potential trace shows less geometric sensitivity (Fig. 3.6). Therefore its robustness towards detecting the tracer propagating through the vagus nerve is better as compared to the needle-shaped and the plate-shaped tracer detector candidates. The j-hook, however, gives the best response. Its surface that detects the electric potential trace is more (Fig. 3.7) and it is less sensitive to changes in position.

Based on the above discussions, it is clear that the j-hook design satisfies both of the design criteria better than any of the other proposed trace detector candidates studied here. It is least likely to cause any damage to the nerve and it has the best robustness towards the detection of the trace propagating through the nerve. Therefore, the j-hook was selected to be used as

the trace detector for the action potential trace propagating through the vagus nerve.

3.3 COMSOL Simulation of Action Potential Detection Using J-Hook Tracer Detector

3.3.1 Geometry

The typical j-hook tip diameter is 5 mm [2, 3]. A j-hook was modeled in COMSOL Multiphysics using a torus geometrical primitive, a 4th order quartic polynomial shape that looks like a donut (Fig. 3.8).

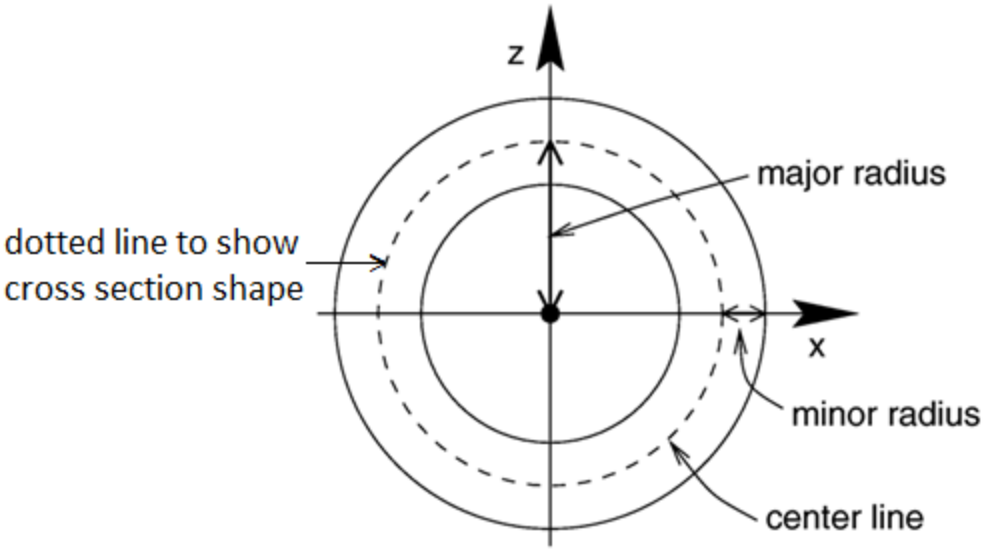

Fig.3.8. Torus [4].

The torus geometry, representing the j-hook tracer detector, is modeled having a major axis radius of 2 mm, minor axis radius of 0.5 mm and revolution angle of 180° (Fig. 3.9). The vagus nerve model developed in Chapter 2 is used as a test bed here to study the simulation of action potential detection using the j-hook tracer detector probe. A series of studies was conducted to measure the sensitivity of the probe to distance from the nerve.

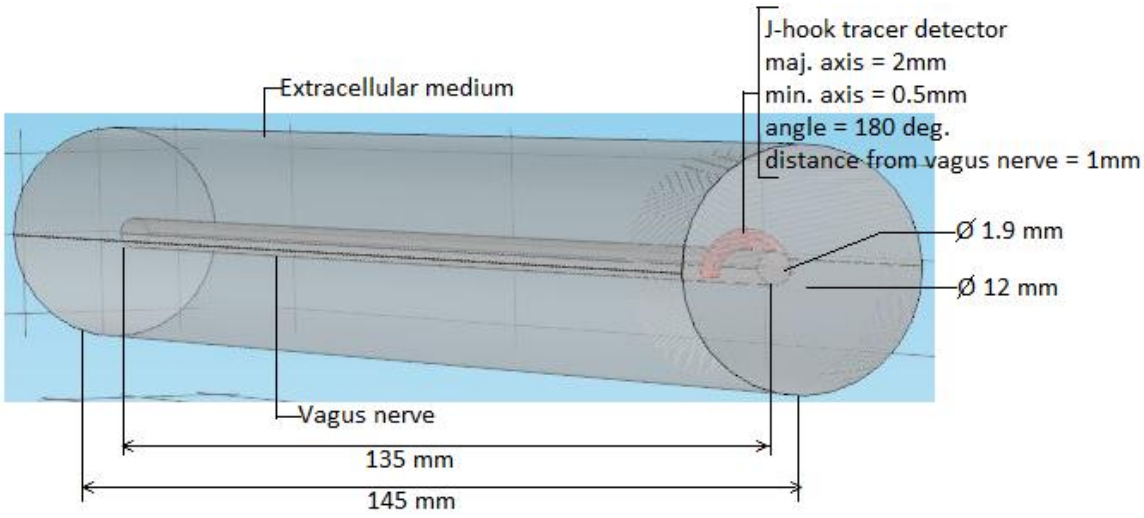

Fig.3.9. J-Hook tracer detector (shown in red) geometry and positioning w.r.t vagus nerve model.

3.3.2 Material

Copper is used in the j-hook tracer detector design. It is same as the material used to design the stimulating cuff. The predefined material contents of copper can be found in Table 2.4.

3.3.3 Sub-domain Settings & Boundary Conditions

The j-hook tracer detector is positioned near the vagus nerve to detect the action potential that has been generated by the applied electrical potential and is propagating through the length of the vagus nerve. Therefore, it is a part of the vagus nerve model and uses the sub-domain settings and boundary conditions that were previously defined (Chapter 2) for the vagus nerve model.

3.3.4 Meshing

For the j-hook tracer detector, a user-controlled mesh has been employed with tetrahedral shaped mesh elements. It is similar to the one employed for the vagus nerve model. In this case, the smallest element size is chosen (length of the longest edge of the mesh element = 0.003 mm) to obtain most accurate detection of the action potential propagating through the vagus nerve. Fig. 3.10 shows a cross section of the meshed model.

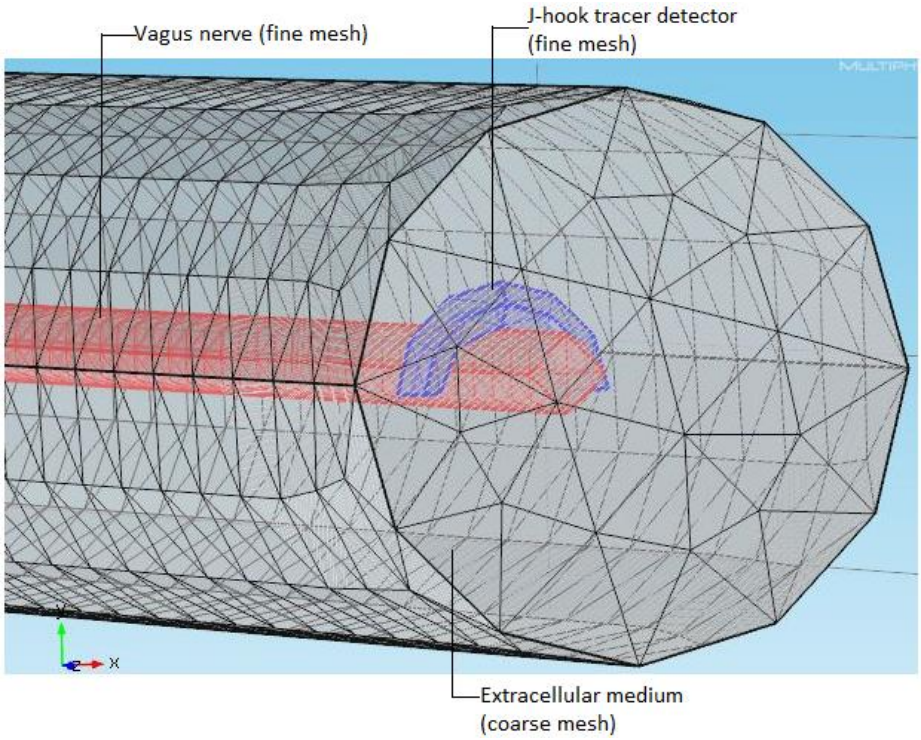

Fig.3.10. Meshed model. The vagus nerve is shown in red and the j-hook tracer detector is shown in blue.

3.3.5 Solver Configuration

The same time dependent solver configuration is used to solve the j-hook tracer detector design as the one used to solve the vagus nerve model. Since the j-hook tracer detector is a part of the vagus nerve model and they are solved simultaneously to detect the action potential propagation through the vagus nerve.

3.3.6 Running the Simulation

The j-hook tracer detector design is executed simultaneously with the vagus nerve model on the Clemson University's primary high performance computing (HPC) resource, the Palmetto cluster. As discussed in the previous chapter, running the simulations on the Palmetto cluster helps save computation time and is therefore the preferred choice to run the complex simulations that are difficult to run on personal desktops/laptops primarily due to RAM limitations.

3.4 Action Potential Detection by the J-Hook Tracer Detector

The j-hook tracer detector is used as a probe to detect the action potential propagating through the vagus nerve. It has some finite thickness (listed earlier) as a result of which, the action potential detected by it at a point on the surface that's closer to the vagus nerve will have lesser attenuation and greater magnitude as compared to the action potential detected by it at a point on the surface that's further away from the vagus nerve. This concept is shown in Fig. 3.11. To select individual surfaces of the j-hook tracer detector, a boundary point probe is chosen in COMSOL Multiphysics.

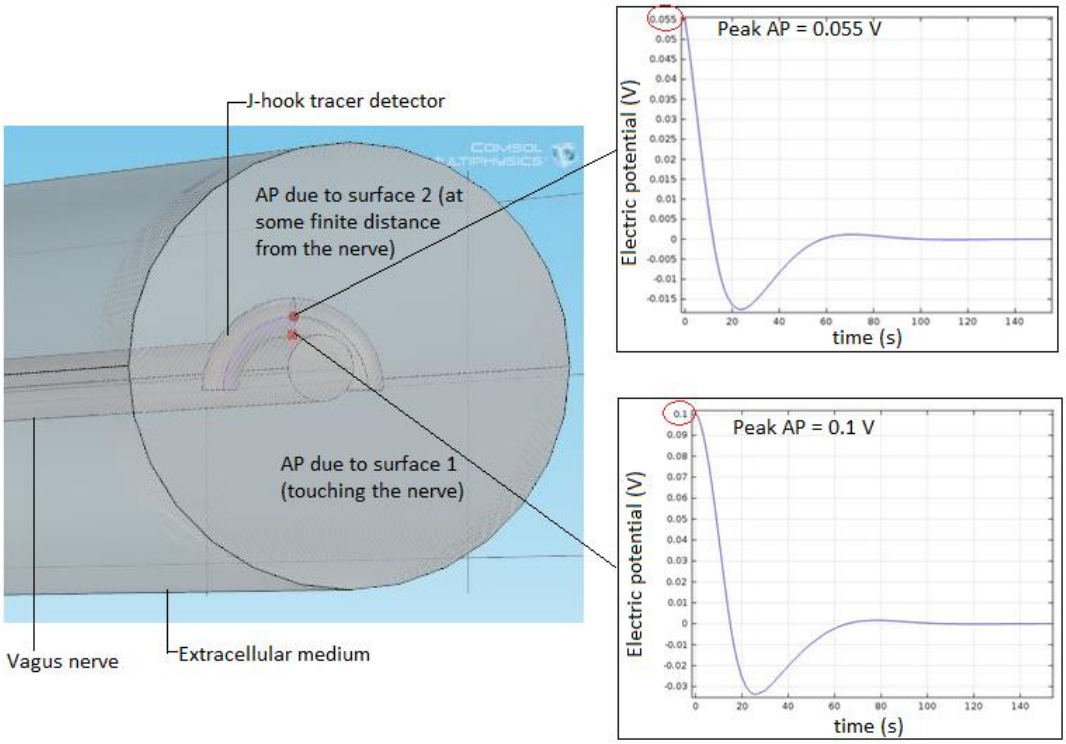

Fig.3.11. Different AP peaks are detected at different surfaces of a j-hook tracer detector due to its finite thickness.

As seen from the figure above, it is not a good idea to study the detection of the action potential at a single point on the surface of the j-hook. Instead, the entire surface should be considered at a time and the average of all the different action potential values detected by the various surfaces of the j-hook should be taken. The averaged action potential would be more close to what the j-hook tracer detector would actually measure in a real-time scenario. In COMSOL Multiphysics, this can be done by selecting the j-hook tracer detector as a domain probe.

Three different case studies were performed to study the effect of moving the j-hook tracer detector away from the vagus nerve on the magnitude of action potential detected.

3.4.1 Case 1: The J-Hook Tracer Detector Touching the Vagus Nerve

Fig. 3.12(a) shows the j-hook tracer detector positioned such that it touches the vagus nerve. The action potential detected by it is shown in Fig. 3.12(b). As discussed above, to make this simulation exercise closely resemble the real-time scenario, the magnitude of action potential presented here is the action potential magnitude averaged over the j-hook tracer detector's domain. Since the j-hook is touching the nerve, one would expect to get an action potential magnitude without any attenuation i.e. the full 0.1 V. But an important thing to note here is that the j-hook is in contact with the nerve at a very small surface. Most of its surfaces are not in direct contact with the vagus nerve and as a result, these surfaces will detect an attenuated value of the action potential. When the average value of action potential due to all surfaces of the j-hook tracer detector is taken, the final action potential has some attenuation as shown in Fig. 3.12(b).

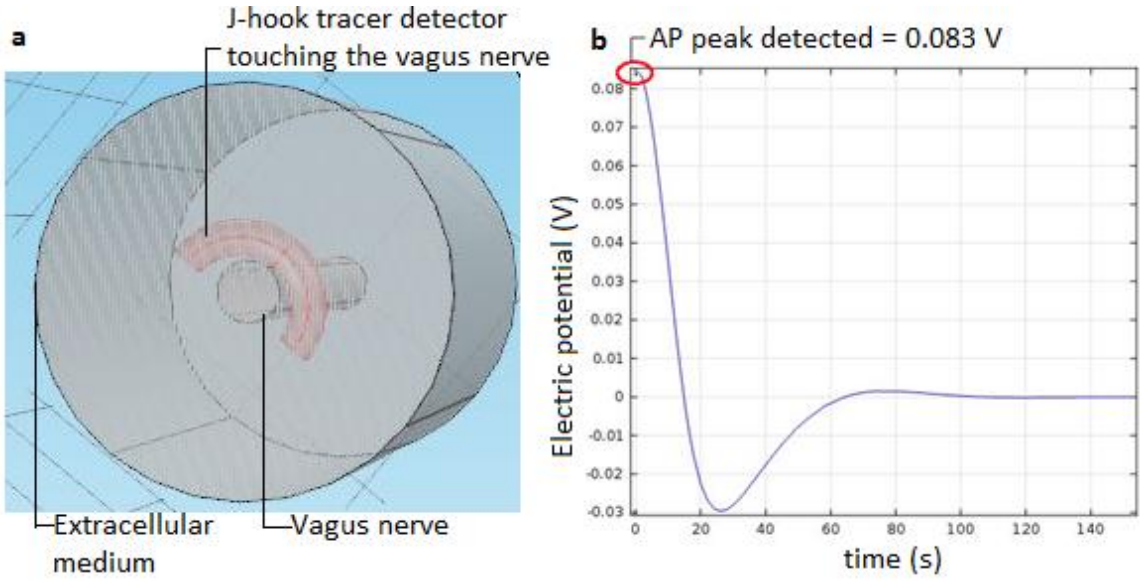

Fig.3.12. (a) J-hook tracer detector positioned such that it touches the vagus nerve. **(b)** AP detected by j-hook tracer detector when touching the vagus nerve.

3.4.2 Case 2: The J-Hook Tracer Detector Positioned 1 mm from the Vagus Nerve

Fig. 3.13 (a) shows the j-hook detector probe positioned at a distance of 1mm from the vagus nerve. The averaged action potential detected by it is shown in Fig 3.13 (b). Here, as expected, the action potential trace has suffered greater attenuation as compared to the previous case since none of the surfaces of the j-hook tracer detector are touching the vagus nerve, and the surfaces that were not touching the vagus nerve in the previous case have become even more distant from the vagus nerve in this case and will detect an even more attenuated value of the action potential. Therefore, the average value

of the action potential due to all surfaces of the j-hook tracer detector will be more attenuated than the previous case (Fig. 3.13(b)).

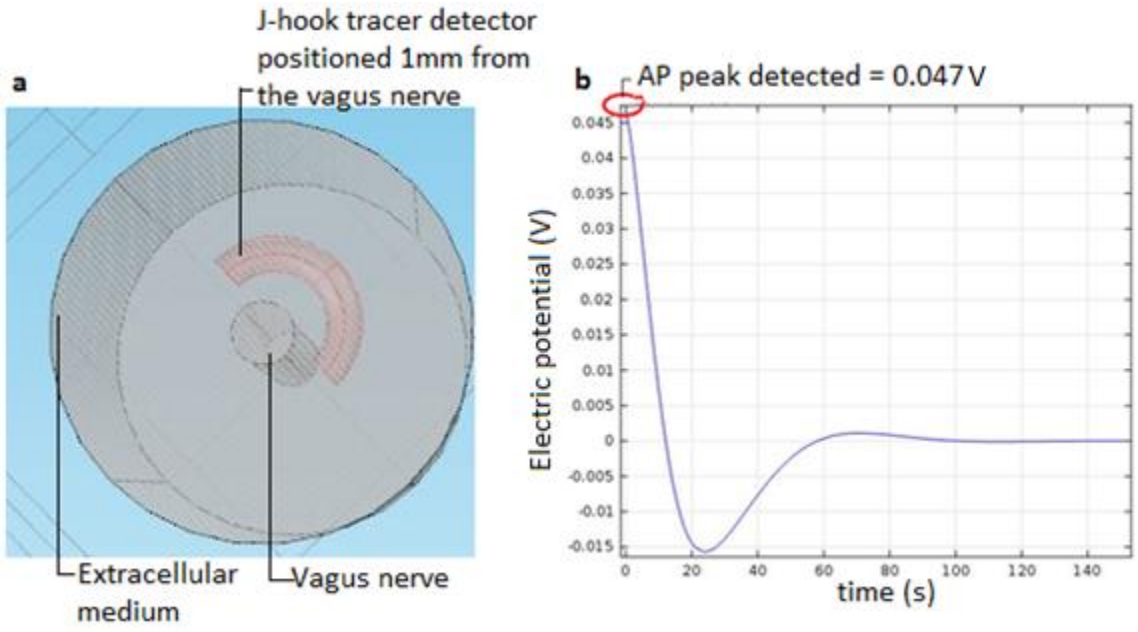

Fig.3.13. (a) J-hook tracer detector positioned 1 mm from the vagus nerve. **(b)** AP detected by j-hook tracer detector positioned 1 mm from the vagus nerve.

3.4.3 Case 3: The J-Hook Tracer Detector Positioned 2 mm from the Vagus Nerve

Fig. 3.14 (a) shows the j-hook detector probe positioned at a distance of 2 mm from the vagus nerve. The averaged action potential detected by it is shown in Fig 3.14 (b). Here the action potential trace has suffered the greatest attenuation out of all three cases since the distances of all the surfaces of the j-hook tracer detector have increased even more in this case and all these will detect an even more attenuated value of the action potential. Therefore, the

average value of the action potential due to all surfaces of the j-hook tracer detector will be even more attenuated than both the previous cases (Fig. 3.14(b)).

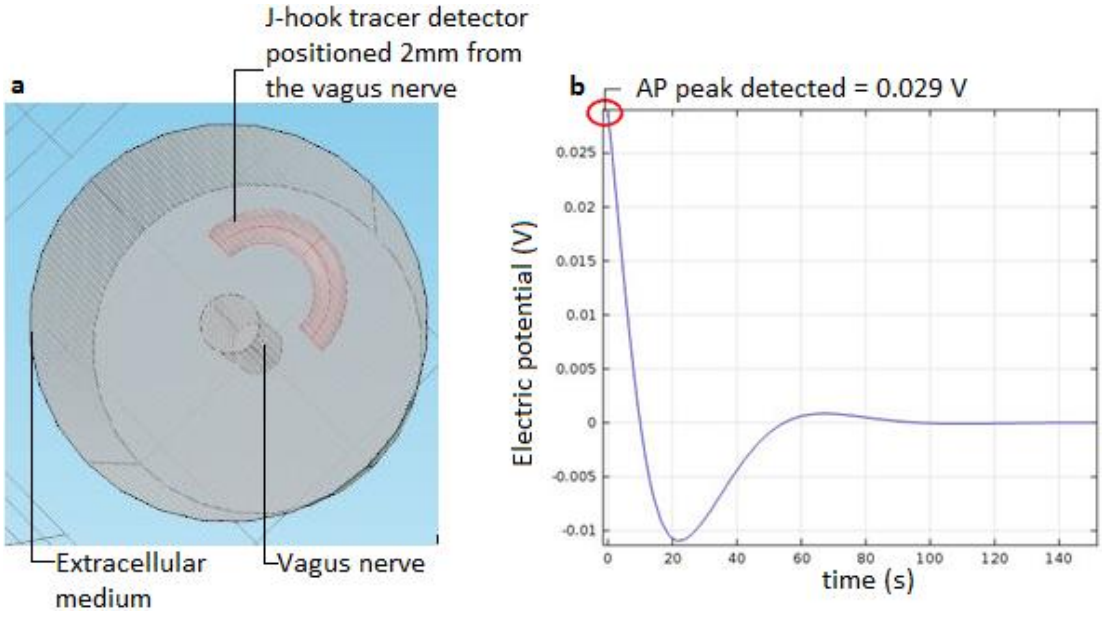

Fig.3.14. (a) J-Hook detector Probe beyond 1 mm from the vagus nerve. **(b)** AP detected by j-hook tracer detector positioned 2 mm from the vagus nerve.

As seen from the results above, it is clear that the j-hook tracer detector probe could be used with the appropriate electronics to detect the action potential propagating through the vagus nerve and can be used by the surgeons performing vagotomy to help them locate the branch of the vagus nerve to cut. The case studies performed above suggest that the action potential magnitude attenuates as the j-hook tracer detector is moved away from the vagus nerve. The studies suggest that the working distance range should be suitable for use in probing the branches of the vagus nerve.

3.4.4 Closeness of the Probe from the Vagus Nerve to Detect Action Potential

In several cases, especially when it comes to actual surgery, it is not advisable to physically touch the nerve with a probe to detect the action potential propagating through it as it might cause damage to the nerve. In this situation it might prove to be really helpful if the surgeon has the knowledge of distance away from the nerve where he/she can detect the correct action potential so that there is no longer a need to physically touch the nerve with the probe.

As a solution to this problem, another interesting study is done. In this study, the attenuation of the peak action potential as the probe is moved away from the vagus nerve is measured and plotted. This helps to determine the distance away from the vagus nerve at which the probe could detect the action potential propagating through the nerve with a fair bit of accuracy and reliability. This in turn does away with the need for the probe to physically touch the vagus nerve.

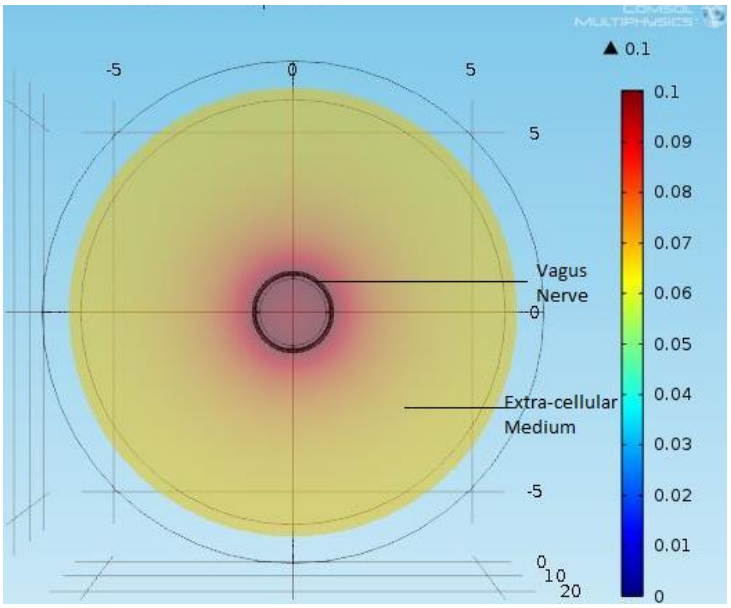

Fig.3.15. AP distribution away from the vagus nerve.

Fig. 3.15 shows the cross-sectional slice of the vagus nerve and the extra-cellular medium. Here the distribution of the action potential is shown as one moves away from the vagus nerve in to the extra-cellular medium. It is quite evident from the figure that the action potential attenuates as we move away from the vagus nerve. This attenuation of action potential is expected and happens due to the electrostatic formulation of the extracellular medium with its material properties.

Fig. 3.16 shows the action potential attenuation plot. Here the attenuation is measured as one moves away from the vagus nerve in to the extracellular medium.

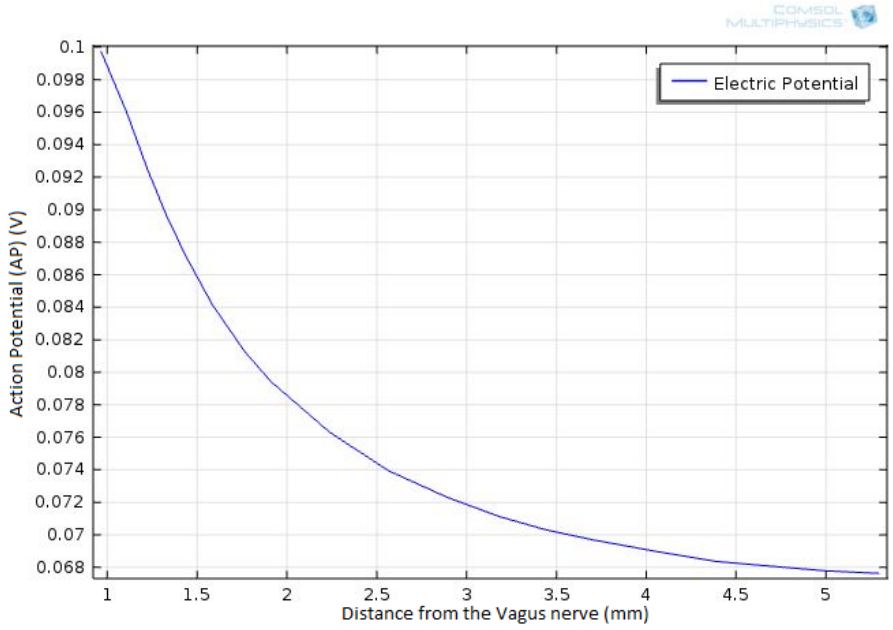

Fig.3.16. AP attenuation plot.

From the attenuation plot, it can be seen that the action potential does not get attenuated a lot when the separation distance of the probe from the vagus nerve is within 1mm. So if the probe is within 1 mm of the vagus nerve, one should be able to detect the action potential propagating through it quite accurately. But if the separation distance between the probe and the vagus nerve is increased beyond 1 mm, the action potential attenuation becomes more prominent and thus the probe might not be able to accurately detect this attenuated action potential.

3.5 The Final System Assembly

Fig. 3.17 (a) below shows all the design elements viz. the tracer signal, the excitation cuffs, the vagus nerve test bed, and the j-hook tracer detector, assembled as a system. The working simulation of this designed system is shown in Fig. 3.17 (b). From the simulation result, it is evident that the designed system meets all the design requirements and performs as expected.

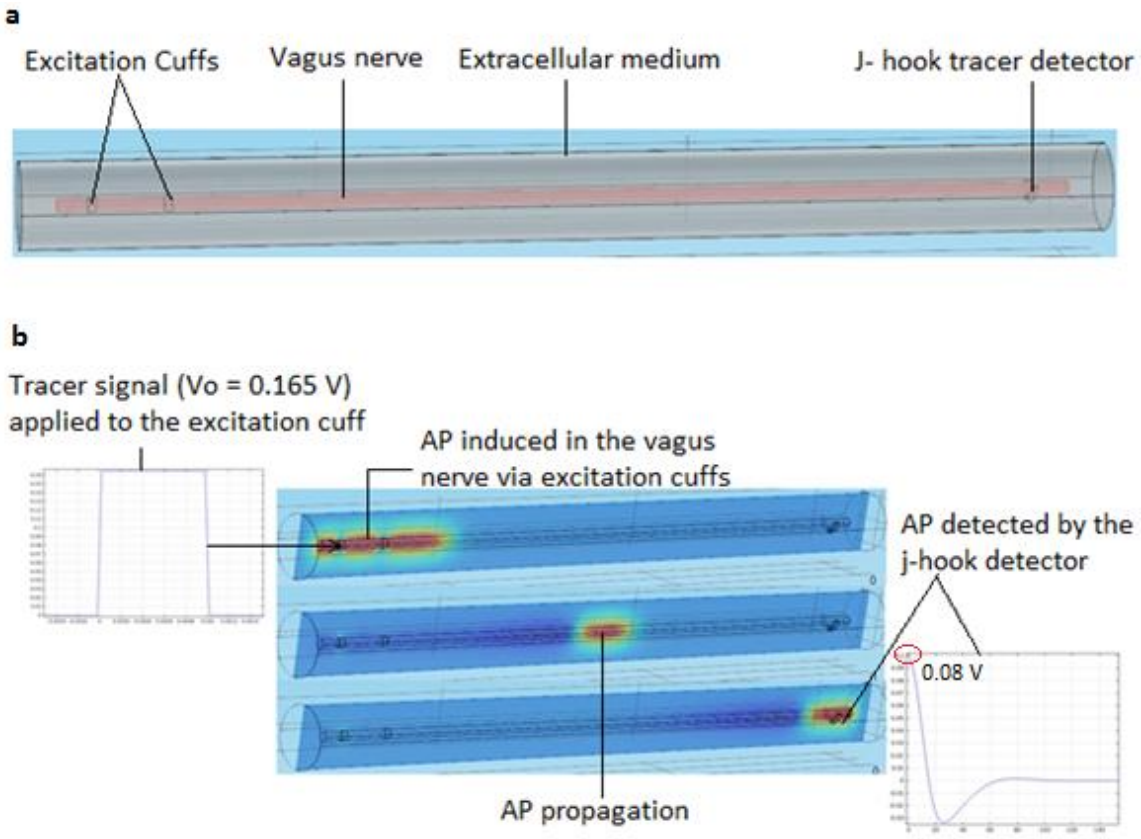

Fig.3.17. The final system assembly: **(a)** Geometrical representation, and (**b)** Simulation.

References

[1] “Laparoscopic Instruments” AESCULAP Surgical Technologies–Product Catalog, http://www.aesculapusa.com/assets/base/doc/doc465_rev_f_laparoscopic_catalog.pdf, last accessed 10/25/2013.

[2] “Monopolar Electrodes with Ceramic Tip”, http://www.pajunkadvantage.com/pdf/Monopolare_Elektroden_GB.pdf, last accessed 10/27/2013.

[3] “Laparoscopic Electrodes”, http://www.conmed.com/endomechanical-instrumentation/lap-electrode.php, last accessed 10/27/2013.

[4] “Torus”, http://www.povray.org/documentation/view/3.7.0/288/, last accessed 10/27/2013.

CHAPTER 4

CONCLUSIONS AND FUTURE SCOPE

The goal of this project was to design a system, which based on the concept of artificial nerve stimulation and nerve signal detection, would enable the surgeons to overcome the major complication of vagotomy surgery of locating the correct branch of the vagus nerve to cut.

The full system design was carried out in two stages using COMSOL Multiphysics 4.3b simulation software to evaluate key design elements. In the first stage, the external electrical stimulation module for a human vagus nerve was developed. A model of a human vagus nerve was created as a test bed for stimulator and detector design. A series of tests were performed on the nerve model, the results indicate the generated action potential propagates through the entire length of the vagus nerve at constant amplitude. This result validates the vagus nerve model by showing that it functions similar to the real vagus nerve. This test bed was used in the design of the tracer signal and the tracer excitation cuffs. The design of the tracer pulse involved fixing the duration of the square pulse to a constant value and varying the amplitude of the pulse (V_0) to get the required action potential peak of 100 mV. After a series of tests with different amplitude values (0.1 V, 0.15 V, and 0.165 V), 0.165 V was selected as the tracer amplitude as it was the minimum pulse amplitude that the

action potential peak of 100 mV was induced in the vagus nerve. In the design of the excitation cuffs, two shapes were considered, half-and full-cuff. A series of simulation tests were performed on both shapes. The tracer excitation full cuffs induce the entire tracer to the vagus nerve test bed whereas the half cuffs transferred a significantly less magnitude of tracer, not sufficient to induce action potential in the vagus nerve. Also, the spread of tracer transferred by the full cuffs was radially symmetric whereas the spread of the tracer transferred by the half cuffs was not. Based on these results, the tracer excitation full cuffs were selected over the tracer excitation half cuffs. The artificial electrical stimulus applied to the vagus nerve model, through stimulating cuff, is able to induce an action potential in it by depolarizing the transmembrane potential beyond its threshold

In the second design stage, the tracer detector probe was created. Different types of laparoscopy instrument end-effectors (needle type, scissor type etc.) were considered, the j-hook type of laparoscopic instrument tip was used as inspiration for the final tracer detector. Based on the results of a series of simulation tests showing that the j-hook satisfied both the design requirements, i.e. it was less likely to damage the nerve as it has a rounded surface and it was less sensitive to change in position and provided maximized detection of the trace signal. Through further simulation trials, it was determined that the distance of the tracer detector probe from the vagus nerve could be as much as 1 mm from the vagus nerve boundary within this distance that the probe would be able

to detect the action potential propagating through the vagus nerve accurately. Beyond this distance, the action potential amplitude attenuates significantly.

The system designed in this project is the first step towards building a system to help surgeons performing the vagotomy surgery find and cut the correct vagus nerve branch. The final utility of the system modeled in this project is to aid the surgeons performing vagotomy on human subjects to correctly locate the vagus nerve branch to cut. The following next steps can be taken to extend this project:

- Work with a surgeon on an animal model to refine the cuff and wire needed to get inside the body to power the cuff.
- Test a possibility to use any tool as a detector.
- Test the trace waveform in presence of noise and find out whether it needs to be more “rich”.

Appendix

Bash Script to Submit Simulation File on the Palmetto Cluster

```
#!/bin/bash
#PBS -N example
#PBS -l select=1:ncpus=10:mpiprocs=10:mem=350gb
#PBS -o stdout.txt
#PBS -e stderr.txt
#PBS -q bigmem
#PBS -l walltime=10:00:00
#PBS -M gbedi@clemson.edu
#PBS -m bea
source /etc/profile.d/modules.sh
module purge
module add comsol/4.2
cd $PBS_O_WORKDIR
comsol batch -inputfile design_1.mph -outputfile design_1_Out.mph
```